MIKE DORMANN

The Design of Broad-Band VLF Receivers with Air-Core Loop Antennas

By
Evans W. Paschal

First Edition, September 1980
Second Edition, May 1988

Contents

Contents

TABLES

ILLUSTRATIONS

ILLUSTRATIONS

0. Introduction

There are many different electromagnetic signals to be found in the very-low-frequency or VLF part of the spectrum.* Naturally-occurring signals include sferics and tweaks, whistlers, chorus and triggered emissions, and plasmaspheric and auroral hiss. Man-made signals range from local power-line fields at harmonics of 50 and 60 Hz to powerful signals from navigation and communications transmitters above 10 kHz.

From a scientific viewpoint, the most important naturally-occurring VLF signal must surely be the *whistler*. A whistler is created when impulsive energy from a lightning stroke (sferic) passes through the ionosphere into the magnetosphere above, and is guided along the earth's magnetic field, returning to ground in the opposite hemisphere. Because of the effects of electrons trapped by the magnetic field, different frequencies are dispersed (travel at different speeds) and the impulsive input wave emerges as a gently falling tone which lasts for a second or two. On occasion whistlers have been heard to descend all the way from 35 kHz down to 300 Hz, though usually they are strongest around 5 kHz. Because dispersion depends on the magnetic field strength (thus identifying the magnetic latitude of the field line followed), while time delay depends on the ionization encountered, whistlers provide a means of monitoring the state of the magnetosphere out to distances as far as five or six earth radii.

Man-made VLF signals are also used in the study of the magnetosphere. The most important source at the moment is the VLF transmitter at Siple Station, Antarctica, run by Stanford University. Two dipole antennas each 42 km (26 miles) long, suspended on short towers above the Antarctic ice sheet, broadcast killowatts of power at frequencies from 2 to 6 kHz to study the interaction of waves and electrons in the magnetosphere. Various naval navigation and communications transmitters in the 10–30 kHz range are used by physicists to monitor sub-ionospheric propagation. A current research topic is the Trimpi event, a brief change in the amplitude and phase of a sub-ionospheric signal due to a temporary pocket of ionization in the lower ionosphere caused by whistler-induced precipitation of energetic electrons from the magnetosphere.

Since the early 1950's, Stanford University has operated broad-band VLF receivers at a number of field stations around the world in an on-going study of VLF radio phenomena.

---

* Strictly speaking, the VLF band covers frequencies in the range 3–30 kHz. However, we shall use the term VLF in a looser sense, including frequencies in the VF (voice-frequency) band at 300 Hz–3 kHz as well. We may occasionally be interested in signals at the upper end of the ELF (extremely-low-frequency) band (30–300 Hz) and at the lower end of the LF (low-frequency) band (30–300 kHz).

Over the years, Stanford's VLF receivers have evolved from early vacuum-tube models to the present solid-state units, with gradual improvements in performance and reliability. The author was responsible for the design of a number of these receivers, and this report is the distillation of various notes he has accumulated.

In some ways the design of a broad-band VLF receiver follows standard audio practice and is similar to, say, the design of a phonograph preamplifier. In other ways receiver design is different; the dynamic range of interesting VLF signals (the ratio of strongest to weakest signal) is much greater than could ever be reproduced from a phonograph record. On the other hand, the signal to be received is an electromagnetic wave and the antenna is a transducer whose impedance is reactive and changes with frequency like HF (high-frequency) antennas. Yet the extreme relative frequency range of 1:1000 calls for different techniques to achieve proper frequency response and noise performance than those used in radio-frequency work.

In this report we shall discuss some of the principles underlying broad-band VLF receiver and antenna design. We shall illustrate the various design principles by applying them to a particular receiver, the Stanford Portable VLF Receiver (1980 model). This is a battery-powered unit that can be used with a number of different antennas of varying sizes and sensitivities. Below are some of the specifications for this receiver and one of its antennas, which will be used in the examples to follow:

56.7 cm Loop Antenna:

Shape	square
Length of Side	56.74 cm
Area	$A = 0.3219$ m^2
Number of Turns	$N = 21$
Wire Diameter	$d = 1.02 \times 10^{-3}$ m (#18 AWG)
Inductance	$L_a = 1.0$ mHy
Resistance	$R_a = 1.0\ \Omega$
Antenna Turnover Frequency	$f_a = 159$ Hz
Normalized Sensitivity	$S_0 = 8.96 \times 10^{-4}$ V Hz$^{1/2}$m^{-1}

Portable VLF Receiver:

Input Transformer Turns Ratio	$m = 22.8$
Receiver Input Resistance	$\approx 1\ \Omega$
Amplifier Input Resistance	$R_{in} = 520\ \Omega$
Amplifier Noise Voltage	$E_n = 2.87 \times 10^{-9}$ V Hz$^{-1/2}$
Amplifier Noise Current	$I_n = 4.44 \times 10^{-13}$ A Hz$^{-1/2}$
Input Turnover Frequency	$f_i = 350$ Hz
Equalized Frequency Range	60 Hz to 60 kHz

1. Design Criteria

1.1 *B vs. E* Field Receivers

Designing a VLF receiver entails at the outset a choice between two complementary approaches: to design a receiver sensitive to the magnetic induction field B, or the electric field E, of the received wave. In some cases, as in the measurement of direction of arrival or wave polarization, it may be necessary to have several antennas and receivers sensitive to different components of both the magnetic and electric fields, but in many cases it is sufficient to measure only one type of field. While this report deals only with magnetic field receivers, I shall summarize here the salient features of each approach. The list below compares the features of magnetic and electric VLF receiving systems.

	Air-Core Loop Receivers	Electric Field Receivers
Antenna Sensitivity	Good. Limited by loop resistance. Worse at low frequencies.	Good. Limited by antenna resistance.
Antenna Response	Proportional to rate of change of B.	Proportional to E.
Sensitivity to Interference	Magnetic interference only. Must be located away from power lines and electric motors.	Electric field interference only. Precipitation static and local thunderstorms a problem, and power lines.
Calibration of Antenna Gain	Simple. Antenna not affected much by nearby structures.	Difficult. May need ground plane. Affected by nearby structures.
Broad-Band Receiver Noise	Good noise figure over at least 10:1 frequency range. Poor at high end in broad-band designs.	Fair at high frequencies. Difficult to get good noise figure at low end.

Magnetic field receivers can use air-core or ferrite-loaded loop antennas, sensitive to the rate of change of the induction field B, or flux-gate (saturating-core), Hall-effect, or SQUID (Superconducting QUantum Interference Device) sensors, sensitive directly to B. Flux-gate and Hall-effect sensors are not usually used above about 10 Hz because of their low sensitivity. SQUID sensors can be used well into the VLF range, but their complexity rules them out except in cases where small antenna size is *the* major consideration. Ferrite-loaded loops are useful where small antenna volume (though not necessarily weight) is

important, but they can suffer from changes in sensitivity with temperature, non-linear response to strong fields, and are somewhat more difficult to calibrate than air-core loops. For absolute measurements of magnetic field strength at frequencies above a few hertz, where antenna size is not a primary concern, air-core loops are the best choice at present.

Electric field receivers in the VLF range invariably use short whip or end-loaded capacitive antennas and very high impedance amplifiers.

1.2 Frequency Response

The first important specification of a receiving system is its gain as a function of frequency, or *frequency response*. The frequency response is important for two reasons. First, we must know the system gain at a given frequency in order to measure the strength of the received signal at that frequency. Second, we must be sure that the gain is not so high at any particular frequency that strong signals will overload the receiver. Naturally-occurring VLF signals have a more or less constant power spectral density from about 300 Hz to 30 kHz. A wide-band receiver with a gain proportional to frequency would tend to overload at high frequencies, or else not have enough gain to detect signals at low frequencies. For ease of measurement and freedom from overloading, a flat frequency response (constant gain *vs.* frequency) is thus desirable for a wide-band receiver.

> *Example:* The Portable VLF Receiver has constant gain for signals from 60 Hz to 60 kHz.

The desired frequency response of the system has important implications for the design of the receiver input. As we shall see, the voltage induced in the loop antenna is proportional to frequency. We must use some technique to compensate for the antenna frequency dependence in order to get an overall flat response.

Note that flat frequency response is not always necessary. In narrow-band receivers frequency response is unimportant and the input design is based on noise considerations alone. For ULF receivers (below, say, 10 Hz) a response proportional to frequency is often desirable, since the power spectral density of ULF signals tends to decrease with increasing frequency.

1.3 Sensitivity

The second important specification of a receiver is its *sensitivity*, or the level of the minimum detectable signal. The minimum detectable signal is limited by random noise generated in the antenna due to thermal fluctuations and by noise added in the receiver. The minimum detectable signal depends on the bandwidth of the measuring instrument, since a wide-band instrument will pass more noise than a narrow-band one. It is convenient to define the *sensitivity* S of the system as the field equivalent of the noise density. That is, a field of amplitude S at the antenna will give a 0 dB signal-to-noise ratio at the receiver output, when measured in a 1 Hz bandwidth. A more sensitive system will thus have a smaller value of S.

The sensitivity of a receiving system is a function of the frequency of the received wave. For air-core loop receivers, S generally decreases (the system becomes more sensitive) as frequency increases.

Note that the sensitivity and the frequency response of the system are independent specifications. They are not directly related to each other.

1.4 Dynamic Range

The *dynamic range* of a receiving system is the ratio of the maximum undistorted signal that can be passed to the minimum detectable signal. The latter is a function of the bandwidth of interest. A large dynamic range is necessary to insure that strong signals will not overload the system while still allowing weak signals to be detected.

> *Example:* The Portable VLF Receiver has a dynamic range of about 130 dB in a 1 Hz bandwidth at a frequency of 5 kHz. This is the ratio of the peak non-distorted signal compared to the rms set noise measured over a 1 Hz band at 5 kHz. The dynamic range is less at other frequencies; the peak level is constant but receiver noise density varies with frequency.

In many cases the limitation on dynamic range in a VLF system is not in the receiver but in ancillary equipment. For instance, if the output of a VLF receiver is recorded on an analog tape recorder, the dynamic range of the tape will be the limiting factor. If the received signal is telemetered from a remote site, a balloon, or a satellite, the telemetry may be the weakest link. In these cases it is important to adjust the signal level from the receiver into the recorder or telemetry transmitter to preserve as much dynamic range as possible.

1.5 Rejection of Interference

Interfering signals passed by the VLF receiver will be indistinguishable at the output from desired signals at the same frequency. If interfering signals are strong enough, they may overload the receiver and generate spurious signal components at other frequencies. A VLF receiving system must keep the level of interference to a minimum. (Of course, one man's signal is another man's noise. A magnetospheric physicist may regard VLF transmitters as sources of interference, while a communications engineer may see whistlers and chorus as unavoidable natural noise.) Following are various types of interference, and steps that can be taken to reduce them:

1. *Hum.* Induction fields from nearby power lines and electrical machinery can create significant interference up to frequencies of 2 or 3 kHz. This interference has a line spectrum which may change slowly with time. The most important factor in reducing hum is the selection of the receiving site. It may be necessary to locate the VLF antenna and receiver some distance from the rest of the station and send signals back over balanced transmission lines. (In this case it is important that ground loops between the station and receiver do not cause additional interference.) Battery operated receivers can be located in quiet areas, but there may be limited power available to operate tape recorders or telemetry. In many cases it will be necessary to sacrifice low-frequency performance and insert a filter in the receiver to attenuate hum noise. The Portable VLF Receiver has a switchable 1 kHz high-pass filter for this purpose.

2. *VLF Transmitters.* Signals from navigation and communications transmitters in the VLF range may be very large, and can overload the receiver and generate spurious intermodulation components in the receiver output. In very sensitive systems it may be necessary to use notch or low-pass filters in the receiver to eliminate this problem. Stanford uses filters with 20 dB attenuation above 10 kHz when making field recordings with its most sensitive receivers. Intermodulation may also occur in the tape recorder if a strong signal saturates the tape. It is important to use tape recorders with constant-current equalization (flat record response) rather than NAB or CCIR equalizations (which emphasize high frequencies).

3. *HF Transmitters.* Signals from HF transmitters may be demodulated at the input of the VLF receiver. This is especially serious in cities, where commercial AM broadcast stations may be a source of interference. To eliminate HF interference it is important to use a well-balanced input design, and to use an electrostatic shield in the receiver input transformer since HF interference is usually capacitively coupled into the receiver. It may help to use an electrostatic shield around the antenna itself.

4. *Wind Noise and Precipitation Static.* Wind noise is caused by signals induced in large loops as they vibrate in the earth's magnetic field because of wind. Very large loops

should not be too taught, so their vibrations will be at frequencies below those of interest. Precipitation static due to rain or snow hitting the antenna can be electrostatically coupled into the receiver. Shielding in the input transformer and/or around the loop can eliminate this problem.

2. Circuit Analysis

It is usually necessary to use a transformer to match the loop antenna to the input amplifier of the VLF receiver. The performance of receivers with realizable transformers is covered in Sections 2.7–2.9, but for the moment we shall assume that we have an ideal transformer. This simplifies the input circuit analysis considerably and allows us to concentrate on the fundamental principles involved in the input design.

2.1 Loop Antenna Model

An equivalent circuit for an air-core loop antenna is shown in Figure 2.1.

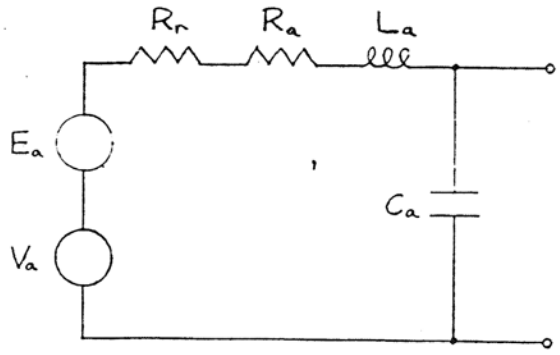

Figure 2.1. Loop antenna equivalent circuit.

V_a is a signal generator representing the antenna voltage due to an incident wave. E_a is a noise generator representing the thermal noise of the antenna.* L_a and R_a are the antenna low-frequency inductance and resistance. R_r is the radiation resistance. C_a is the loop distributed capacity. The calculation of L_a, R_a, and C_a is covered in Chapter 3.

Another important loop parameter is the *antenna turnover frequency* f_a, defined as

$$f_a = \frac{R_a}{2\pi L_a}. \tag{2.1}$$

f_a is the frequency where the reactance of L_a equals the dc resistance R_a. Below this frequency the loop is primarily resistive, while above f_a the loop is primarily inductive.

Since practical VLF loops are quite small compared to the wavelength of the incident waves, the radiation resistance of the antenna is much smaller than the other impedances.

* We shall use V for signal voltages and E for noise voltages. However, E_w will be the incident wave electric field.

Watt [1967] gives a formula for R_r as

$$R_r = 7.72 \times 10^{-30} f^4 N^2 A^2 \qquad [\Omega] \tag{2.2}$$

where N is the number of turns and A is the area of each turn.

Example: Consider a loop made of 21 turns of #18 copper wire wound on a square form 56.7 cm on a side. This is one of the standard antennas used with the Portable VLF Receiver. This loop has the following circuit elements:

$$\begin{aligned} R_a &= 1.0\ \Omega \\ L_a &= 1.0\ \text{mHy} \\ R_r &= 4 \times 10^{-8}\ \Omega \text{ at } f = 100\ \text{kHz} \\ C_a &= 800\ \text{pF} \\ F_a &= 159\ \text{Hz}. \end{aligned}$$

Even at 100 kHz, R_r is negligible compared to R_a, and we can safely ignore it. C_a is also relatively small and can be ignored.

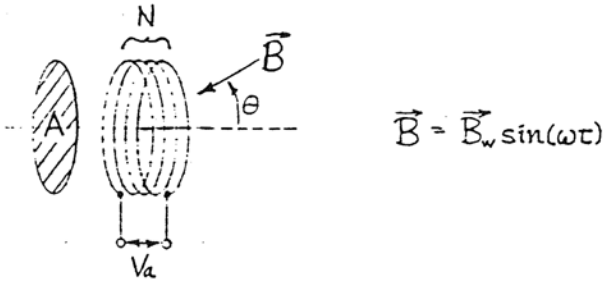

Figure 2.2. Voltage induced in loop.

The voltage V_a induced in the loop depends on the field B passing through the loop, as shown in Figure 2.2. Since VLF loops are very small compared to the wavelength of the incident wave, at any given moment the magnetic field B is essentially uniform across the area of the loop. We have, then

$$\begin{aligned} V_a &= -N \frac{\partial}{\partial t} \int \vec{B} \cdot d\vec{A} \\ &= j\omega N A B_w \cos(\theta) \\ &= j\omega N A B_w \quad \text{for} \quad \theta = 0 \end{aligned} \tag{2.3}$$

where we have assumed a sinusoidal field of magnitude B_w and radian frequency $\omega = 2\pi f$, incident at an angle θ from the axis of the loop. In the following we shall be concerned

with the response of the loop to an appropriately oriented field and we shall omit the term $\cos(\theta)$.

We shall often refer to the response of the receiver in terms of the equivalent electric field E_w of the incident wave, rather than its magnetic field B_w, as many engineers are relatively unfamiliar with magnetic units. In free space the two are related by

$$E_w = cB_w \tag{2.4}$$

where E_w and B_w are in the MKS units of volts per meter (V m^{-1}) and teslas (T), respectively, and where $c = 2.998 \times 10^8$ m s^{-1} is the speed of light. Other commonly encountered units for B_w are the gauss (G) and gamma (γ). In free space,

$$\begin{aligned} 1 \text{ volt per meter} &= 3.34 \times 10^{-9} \text{ tesla} \\ &= 3.34 \times 10^{-5} \text{ gauss} \\ &= 3.34 \text{ gamma.} \end{aligned}$$

However, we must remember that the loop responds to the magnetic field, not the electric field, of the wave. Depending on the location of the antenna, the local value of E_w may not be that given by Equation (2.4).

The noise generator E_a represents the voltage present in the loop in the absence of any magnetic field. It is essentially the thermal noise of the loop resistance R_a,* and its rms value is given by

$$\langle E_a \rangle = (4kT\Delta f R_a)^{1/2} \qquad \text{[V rms]} \tag{2.5}$$

where $k = 1.38 \times 10^{-23}$ J K^{-1} is Boltzmann's constant, T is the temperature in kelvins (that is, °C+273), and Δf is the bandwidth over which the noise voltage is measured. At room temperature, $4kT = 1.61 \times 10^{-20}$ joule. We have written the value of noise voltage as $\langle E_a \rangle$ to emphasize that it is a time average; the actual voltage as a function of time is a random process. We shall drop this notation hereafter, remembering that each noise source is statistically random, and that only its mean squared value and not its instantaneous value is well-defined.

---

* Note that we usually consider R_a to be the dc resistance of the loop. In fact, because of the skin effect (the tendency of the magnetic field due to current flowing inside a wire to push the current out of the interior and toward the surface) and the proximity effect (a similar force due to currents flowing in other conductors in a multi-turn loop) the resistance of a loop increases at higher frequencies, resulting in increased noise. In practice this is not a problem because total receiver noise at high frequencies is dominated by other noise sources.

Note that T is the temperature of the wire. Since R_r is small compared to R_a, the loop noise does not depend on the temperature of the medium, as is often true with antennas at higher frequencies.

In the following discussion we shall be concerned with the *noise density* or spot noise of various noise sources, rather than their broad-band values. Noise density is calculated using a bandwidth of $\Delta f = 1$ Hz. The noise density of R_a is then

$$E_a = (4kTR_a)^{1/2} \qquad [\text{V Hz}^{-1/2} \text{ — noise density}]. \tag{2.6}$$

If the noise density is flat (independent of frequency), as is the noise source E_a, we can find the rms noise voltage over a different bandwidth Δf by multiplying Equation (2.6) by $\sqrt{\Delta f}$. Noise power (or E_a^2) rather than noise voltage is proportional to bandwidth.

Example: For the 56.7 cm standard loop we have $R_a = 1\ \Omega$, giving $E_a = 1.27 \times 10^{-10}$ V Hz$^{-1/2}$.

2.2 Antenna Sensitivity

In Section 1.3 we defined the *sensitivity* S of a receiving system as the field equivalent of the noise density; that is, the amplitude of an incident wave which would give an output response equal to the output signal due to noise in a 1 Hz bandwidth.* The *antenna sensitivity* S_a is the field strength of the weakest signal that could be received in a 1 Hz bandwidth if the antenna were connected to a perfect (*i.e.*, noiseless) amplifier; the field equivalent of the antenna noise density. The signal voltage induced in the antenna is given by Equation (2.3), and the noise voltage by Equation (2.6). Combining these and solving for B_w we find the antenna sensitivity is

$$S_a = \frac{(4kTR_a)^{1/2}}{\omega NA} \qquad [\text{T Hz}^{-1/2}], \tag{2.7}$$

or

$$S_a = \frac{c(4kTR_a)^{1/2}}{\omega NA} \qquad [\text{V Hz}^{-1/2}\text{m}^{-1}]$$

in terms of the equivalent electric field. The antenna sensitivity S_a decreases with frequency (that is, the antenna becomes more sensitive) as $1/f$. It is convenient to define a frequency-independent quantity for comparing the performance of different antennas. We define the *normalized antenna sensitivity* S_0 as

$$S_0 = \frac{(4kTR_a)^{1/2}}{2\pi NA} \qquad [\text{T Hz}^{1/2}], \tag{2.8}$$

or

---

* This is somewhat unfortunate terminology, since a *more sensitive* system has a *smaller sensitivity* S. However, it is easier to write *sensitivity* S than *field-equivalent noise density* S.

$$S_0 = \frac{c(4kTR_a)^{1/2}}{2\pi NA} \qquad [\text{V Hz}^{1/2}\text{m}^{-1}].$$

The actual sensitivity of the antenna at any given frequency is then

$$S_a(f) = S_0/f. \tag{2.9}$$

Note that the antenna sensitivity depends on the antenna size and resistance, but does not depend on the antenna inductance L_a or turnover frequency f_a. See Chapter 3 for the calculation of sensitivity in antenna design.

Example: The 56.7 cm standard loop has a normalized sensitivity of $S_0 = 8.96 \times 10^{-4}$ V $\text{Hz}^{1/2}\text{m}^{-1}$.

2.3 Amplifier Model

Figure 2.3 shows the model we shall use for the input amplifier in the VLF receiver. The amplifier has an input resistance R_{in} and a voltage gain G. The amplifier is shown connected to a source with noise voltage generator E_s and impedance Z_s. Note that $Z_s = R_s + jX_s$ is in general a complex impedance. For instance, we will often be concerned with a loop antenna with impedance $Z_a = R_a + jX_a = R_a + j\omega L_a$.

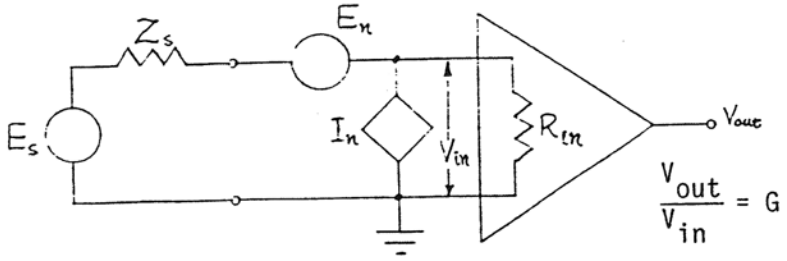

Figure 2.3. Amplifier equivalent circuit.

We have represented the noise of the amplifier by using two noise generators, voltage generator E_n and current generator I_n, connected to the amplifier input. No matter where the noise actually originates in the amplifier, it can be referred to the input in this manner; this is a general representation for an amplifier at a given frequency. We shall assume that E_n and I_n are statistically uncorrelated. This may not be strictly true for all amplifiers, but it is usually a good approximation. E_n and I_n are also uncorrelated with the source

noise E_s. We find that the mean square value* of the output noise is

$$E_{out}^2 = (E_s^2 + E_n^2 + I_n^2 Z_s^2) \frac{R_{in}^2}{|R_{in} + Z_s|^2} G^2. \tag{2.10}$$

It will be convenient later on to use the concept of the *noise referred to the source.* We replace all the circuit noise generators with a single generator at the source, E_{ni}, that gives an equivalent output noise voltage, as shown in Figure 2.4.

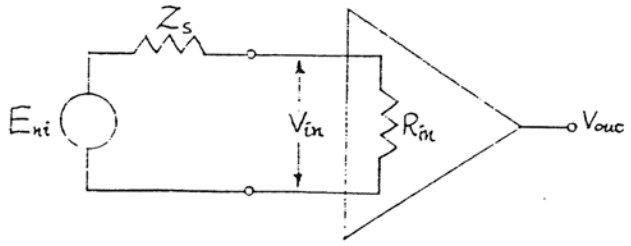

Figure 2.4. Noise referred to the source.

We find

$$E_{ni}^2 = E_s^2 + E_n^2 + I_n^2 Z_s^2. \tag{2.11}$$

This is a useful transformation because it is easier to see how much the performance of the circuit is degraded by amplifier noise. If the amplifier were noiseless we would have $E_{ni}^2 = E_s^2$. We never achieve this, of course, but a good amplifier will come close.

* Note that it is the powers (or voltages-squared) of uncorrelated noise sources in series that are added together, not the voltages themselves. See *Motchenbacher and Fitchen* [1973] for further discussion of noise models.

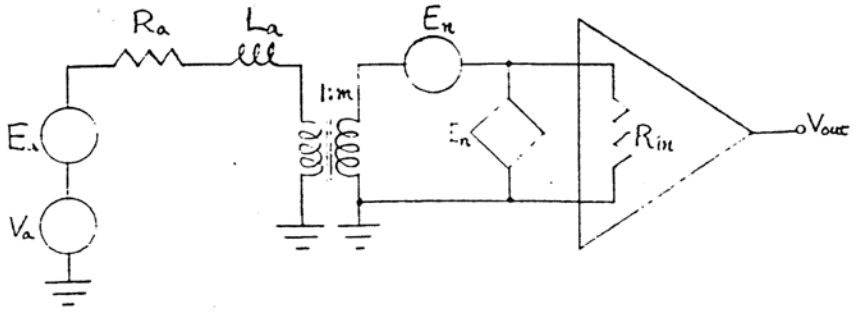

Figure 2.5. Receiver input equivalent circuit: ideal transformer.

2.4 Receiver Frequency Response: Ideal Transformer

Figure 2.5 shows the equivalent circuit of the input of the VLF receiver. A transformer with a turns ratio of 1:m is used to match the antenna to the input amplifier. We shall assume for the moment that this is an ideal, lossless transformer. (Real transformers are covered in Sections 2.7–2.9.) Ignoring for the moment the noise generators, we find that the voltage at the output of the amplifier due to the signal voltage V_a induced in the antenna is

$$V_{out} = \frac{mV_aR_{in}G}{R_{in} + m^2Z_a} \tag{2.12}$$

where $Z_a = R_a + j\omega L_a$. Substituting the expression for V_a from Equation (2.3) we have

$$V_{out} = \frac{j\omega NAB_w mR_{in}G}{R_{in} + m^2R_a + j\omega m^2L_a} \tag{2.13}$$

or

$$V_{out} = \frac{NAB_wR_{in}G}{mL_a} \cdot \frac{f}{f - jf_i} \tag{2.14}$$

where

$$f_i = \frac{R_a + R_{in}/m^2}{2\pi L_a}. \tag{2.15}$$

The quantity f_i is the *input turnover frequency,* defined as the frequency where the reactance of the loop is equal to the resistance of the input circuit. Note that f_i is always greater than f_a (Equation (2.1)). Below f_i, the reactance ωL_a is small compared to $R_a + R_{in}/m^2$ and the output voltage for a constant field increases with increasing frequency. Above f_i, ωL_a is large compared to the resistance of the circuit and the increase in loop reactance compensates for the increase in V_a with frequency, giving an output independent of frequency. We can adjust f_i by changing the turns ratio of the input transformer. From noise considerations, however, we shall often choose m so that $R_{in}/m^2 \approx R_a$, giving $f_i \approx 2f_a$.

For broad-band reception it is best to operate at frequencies above f_i so that the output of the receiver is proportional to the amplitude of the incident wave but independent of its frequency (see Section 1.2). Note how we achieve this flat frequency response: we rely on the increasing reactance ωL_a of the loop antenna. Even though the signal emf induced in the loop increases with frequency, the loop reactance increases at the same rate. As long as the impedance in the input circuit is dominated by this reactance the frequency response will be flat. Because of this, a wide-band VLF receiver designed for use with loop antennas has a very low input impedance ($\sim R_a$) as seen at the antenna terminals. It is possible to compensate for the fall-off in response below f_i by frequency equalization at some later stage in the receiver; however, because of dynamic range considerations the band over which equalization can be used may be limited.

> *Example:* Consider the 1 Ω/1 mHy standard loop, with $f_a = 159$ Hz. We can adjust the input transformer so that the input impedance of the Portable VLF Receiver is $R_{in}/m^2 = R_a = 1\ \Omega$, giving $f_i = 318$ Hz. The receiver will then have a flat frequency response to signals above 318 Hz, but will give less output for signals below that frequency. In the Portable VLF Receiver equalization is used to extend the frequency of flat response down to about 60 Hz, or $0.2 f_i$.

Note that we have not tried to tune the antenna to maximize the transfer of signal power to the amplifier. There is no way to achieve this over the wide relative frequency range (say 60 Hz to 60 kHz, a ratio of 1:1000) we wish to cover. Wide-band receiver design is quite different from narrow-band design, where adding a parallel capacitance $C = 1/\omega^2 L_a$ to counteract the antenna inductance in a small range about the frequency ω would be appropriate.

2.5 System Sensitivity: Ideal Transformer

Because any practical amplifier will add some additional noise to the signals from the antenna, the sensitivity of a VLF receiver as a whole will be worse than that of its antenna alone. Our goal is to make the amplifier noise contribution as small as possible. Using the equivalent input circuit in Figure 2.5 we find that the output voltage due to noise is

$$E_{out}^2 = m^2 \left(E_a^2 + \frac{E_n^2}{m^2} + I_n^2 m^2 Z_a^2 \right) \frac{R_{in}^2}{|R_{in} + m^2 Z_a|^2} G^2 \tag{2.16}$$

where $Z_a = R_a + j\omega L_a = R_a(1 + jf/f_a)$. Combining this with Equation (2.13) and solving for B_w we find that the *system sensitivity* S_{sys} is given by

$$S_{sys} = \left(E_a^2 + \frac{E_n^2}{m^2} + I_n^2 m^2 Z_a^2 \right)^{1/2} \frac{1}{\omega N A} \qquad [\text{T Hz}^{-1/2}]. \tag{2.17}$$

At low frequencies, the sensitivity S_{sys} increases with decreasing frequency (*i.e.*, the receiver becomes less sensitive). At high frequencies, the term $I_n^2 m^2 Z_a^2$ dominates (since $Z_a^2 \simeq \omega^2 L_a^2$) and the sensitivity S_{sys} approaches a constant minimum value. We have assumed that the amplifier noise sources E_n and I_n are independent of frequency. This is a good approximation in our case, but not strictly true.

2.6 Receiver Noise Figure: Ideal Transformer

While Equation (2.17) accurately describes the noise behavior of our model receiver, we can get a clearer picture of receiver performance if we use the concept of receiver noise factor. The *noise factor* F is defined as

$$F = \frac{\text{signal/noise ratio at input}}{\text{signal/noise ratio at output}}$$

or

$$F = \frac{\text{total noise power at input}}{\text{noise power at output due to input noise}}. \tag{2.18}$$

We can also express F in decibels, calling the quantity the *noise figure* NF,* as

$$NF = 10 \log(F). \tag{2.19}$$

* The noise factor F is sometimes also called the noise figure. We shall follow convention in this report, but having different names for F and NF is somewhat arbitrary since they both refer to the same parameter. Using one name would be no more confusing than with amplifier gain, which is specified either as a ratio (of voltages, say), or equivalently in decibels, depending on the context.

From Equation (2.16) we see that the noise factor of our receiver is

$$F = \frac{E_a^2 + E_n^2/m^2 + I_n^2 m^2 Z_a^2}{E_a^2}$$
$$= 1 + \frac{E_n^2}{m^2 E_a^2} + \frac{I_n^2 m^2 Z_a^2}{E_a^2}. \tag{2.20}$$

F is also given conveniently by

$$F = \frac{E_{ni}^2}{E_a^2}. \tag{2.21}$$

The noise factor is a measure of the amount of additional noise the amplifier adds to the input signal. Note that the noise factor of a perfect, noiseless amplifier is 1 (noise figure $NF = 0$ dB). The noise figure of our receiver is constant at low frequencies, but rises at high frequencies as Z_a becomes larger. We can write the system sensitivity in terms of the antenna sensitivity and amplifier noise factor in the following simple way

$$S_{sys} = S_a\sqrt{F} = S_0\sqrt{F}/f. \tag{2.22}$$

Equation (2.22) is useful because it allows us to separate the noise effects of the antenna and the amplifier. In Chapter 3 we shall design several different antennas with the same impedance but different sensitivities to be used with the Portable VLF Receiver. Using Equation (2.22) we can easily calculate the overall system sensitivity for each antenna. (This approach is only useful for antennas with the same impedance Z_a, since F depends on the source impedance.)

We can separate the constant and frequency-dependent terms of Equation (2.20) using $Z_a = R_a(1 + f^2/f_a^2)$ and we have

$$F = 1 + \frac{E_n^2}{m^2 E_a^2} + \frac{I_n^2 m^2 R_a^2}{E_a^2} + \frac{I_n^2 m^2 R_a^2}{E_a^2} \cdot \frac{f^2}{f_a^2}. \tag{2.23}$$

In a good design, the third term is negligible and can be ignored. Substituting for E_a^2 (Equation (2.6)) we have

$$F \simeq 1 + \frac{E_n^2}{4kTm^2 R_a} + \frac{I_n^2 m^2 R_a^2}{4kT} \cdot \frac{f^2}{f_a^2}. \tag{2.24}$$

We can trade off low and high frequency performance by adjusting the input transformer turns ratio m. A large m gives good performance at low frequencies, but the noise figure deteriorates rapidly at higher frequencies. A small m gives worse performance at

low frequencies, but better performance at higher frequencies. A good choice for most amplifiers is to set the low-frequency noise factor to $F = 2$ ($NF = 3$ dB) by choosing

$$m = E_n/(4kTR_a)^{1/2}. \tag{2.25}$$

This gives fairly good sensitivity at low frequencies while preserving most of the higher frequency performance. In most cases it is much easier to increase the antenna size than to decrease the receiver noise figure in order to improve the overall system sensitivity.

Example: Consider the 56.7 cm loop connected to the Portable VLF Receiver input amplifier through a transformer with an adjustable turns ratio m. We have the following values:

$$\begin{aligned} R_a &= 1.0\ \Omega \\ L_a &= 1.0\ \text{mHy} \\ f_a &= 159\ \text{Hz} \\ S_o &= 8.96 \times 10^{-4}\ \text{V Hz}^{1/2}\text{m}^{-1} \\ R_{in} &= 520\ \Omega \\ E_a &= 1.27 \times 10^{-10}\ \text{V Hz}^{-1/2} \\ E_n &= 2.87 \times 10^{-9}\ \text{V Hz}^{-1/2} \\ I_n &= 4.44 \times 10^{-14}\ \text{A Hz}^{-1/2}. \end{aligned}$$

Figures 2.6 through 2.8 on the following pages show the noise figure, sensitivity, and frequency response of this system for different values of m. In the Portable VLF Receiver, m was chosen to be 22.8.

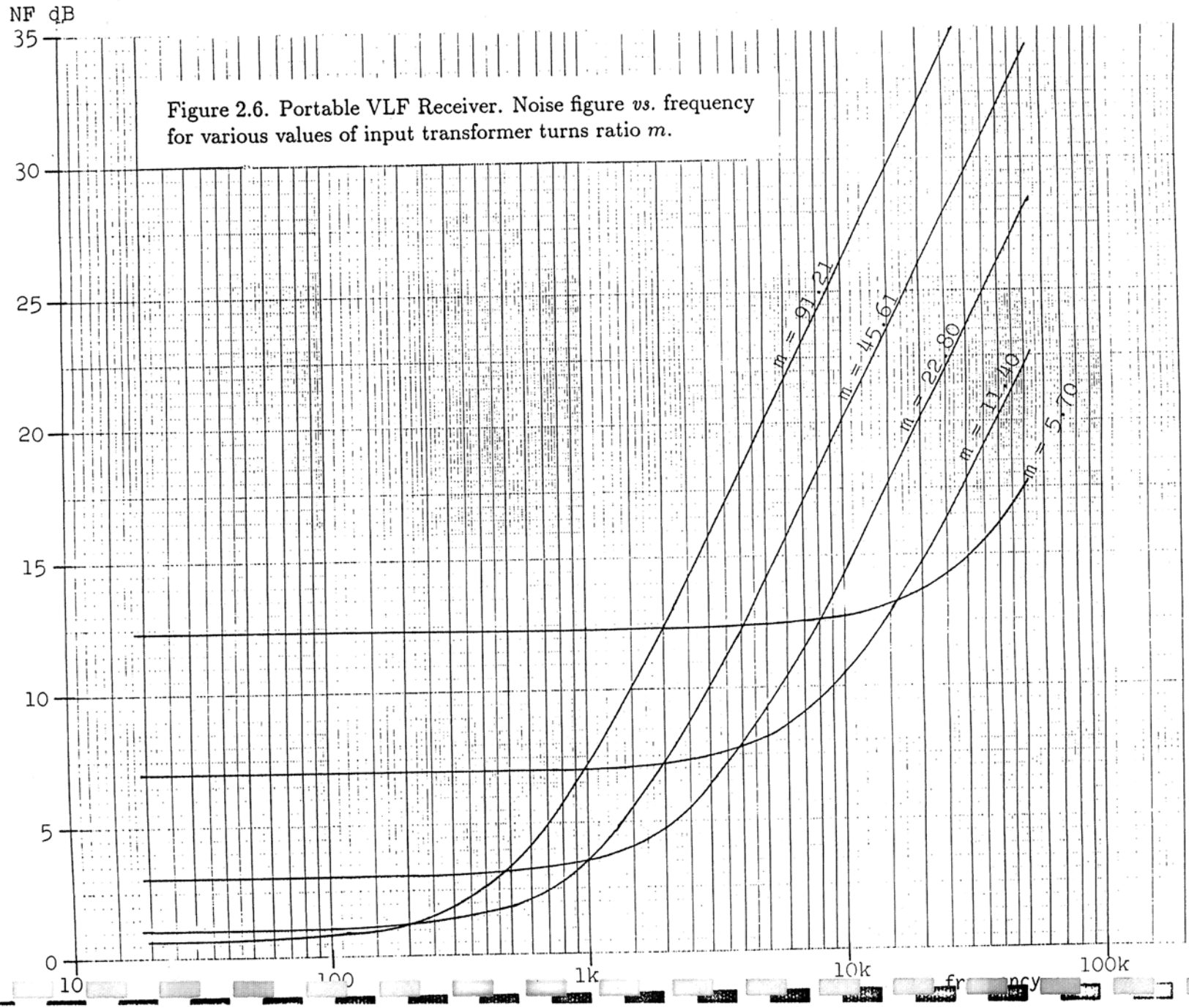

Figure 2.6. Portable VLF Receiver. Noise figure *vs.* frequency for various values of input transformer turns ratio m.

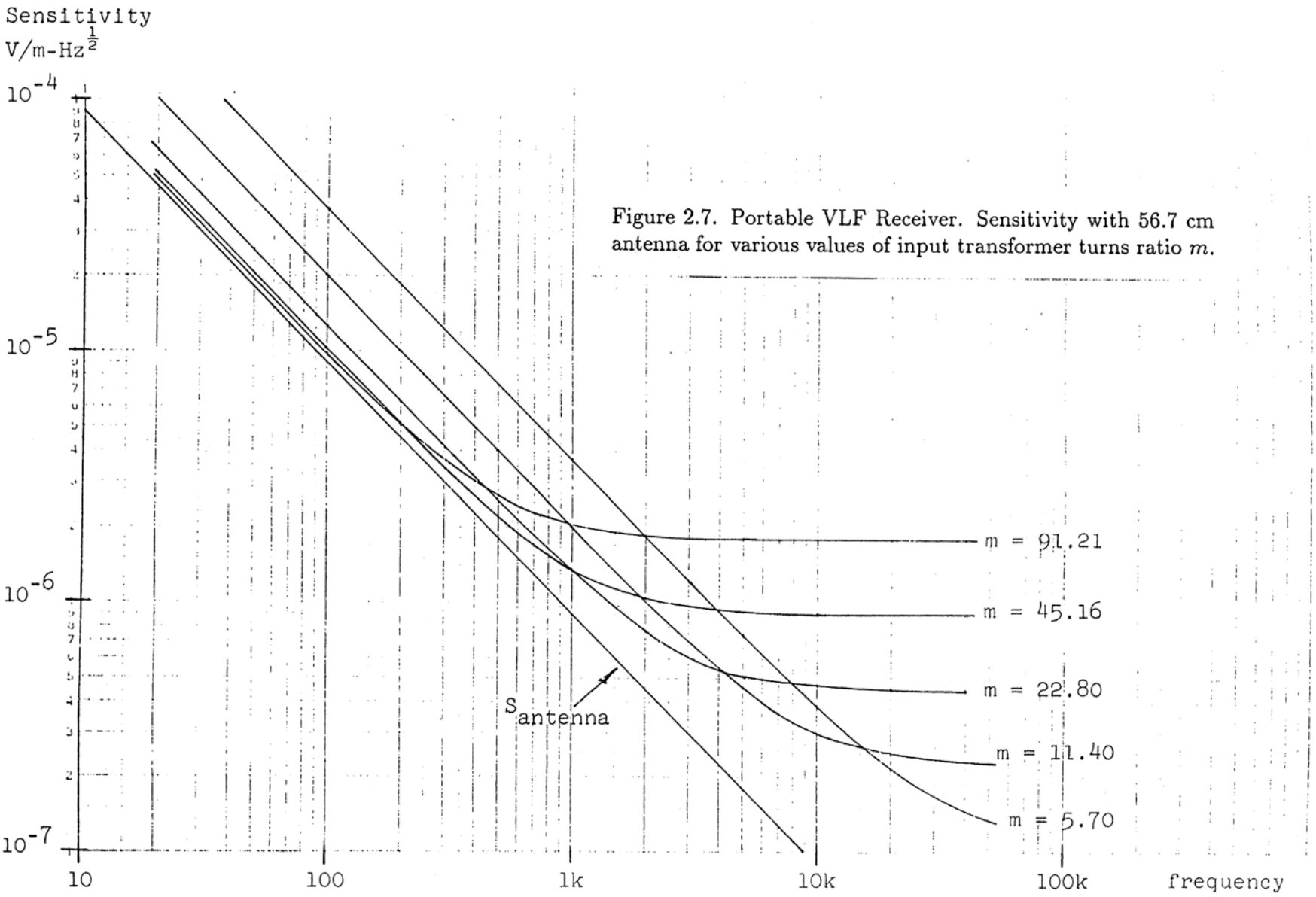

Figure 2.7. Portable VLF Receiver. Sensitivity with 56.7 cm antenna for various values of input transformer turns ratio m.

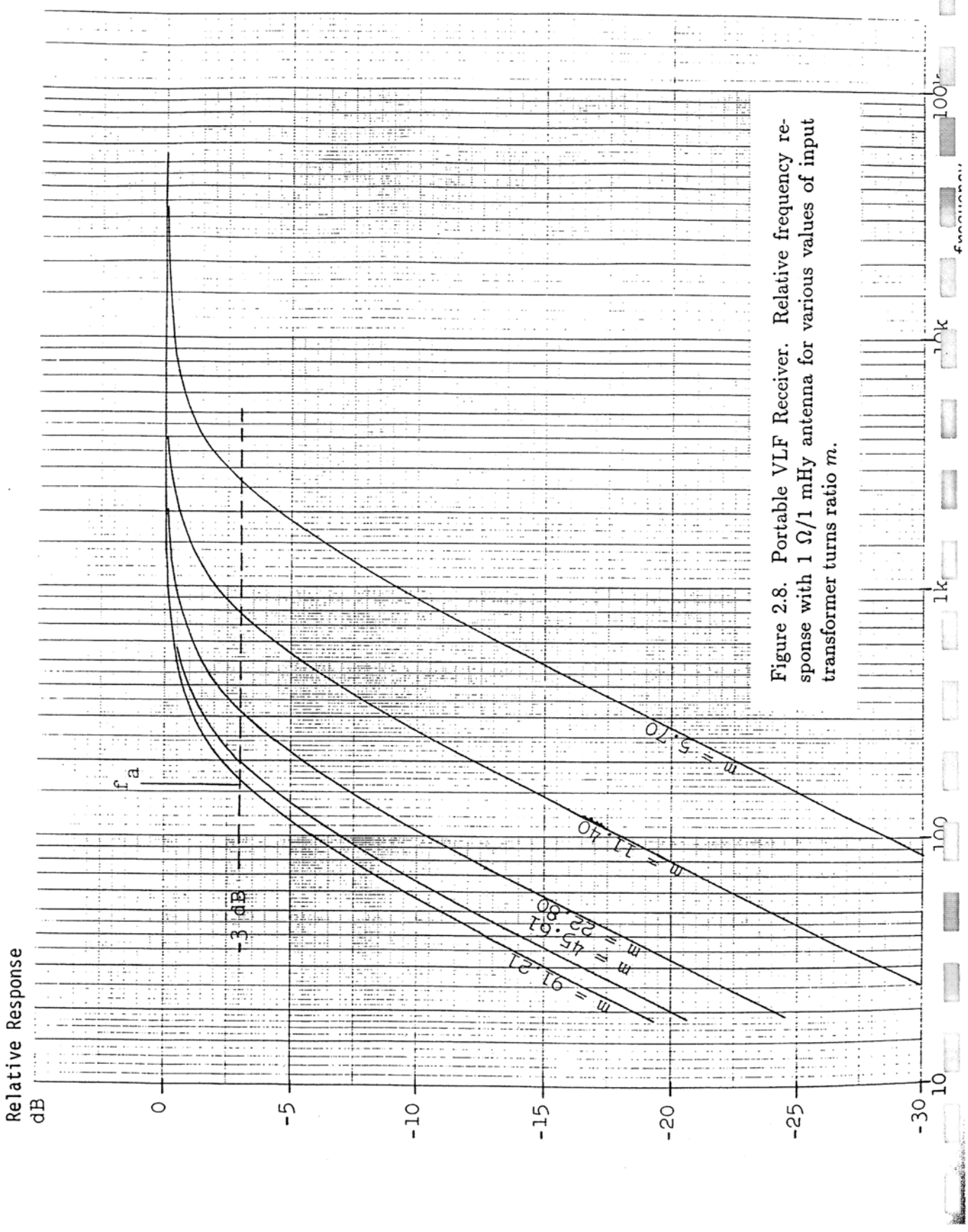

Figure 2.8. Portable VLF Receiver. Relative frequency response with 1 Ω/1 mHy antenna for various values of input transformer turns ratio *m*.

2.7 Transformer Model

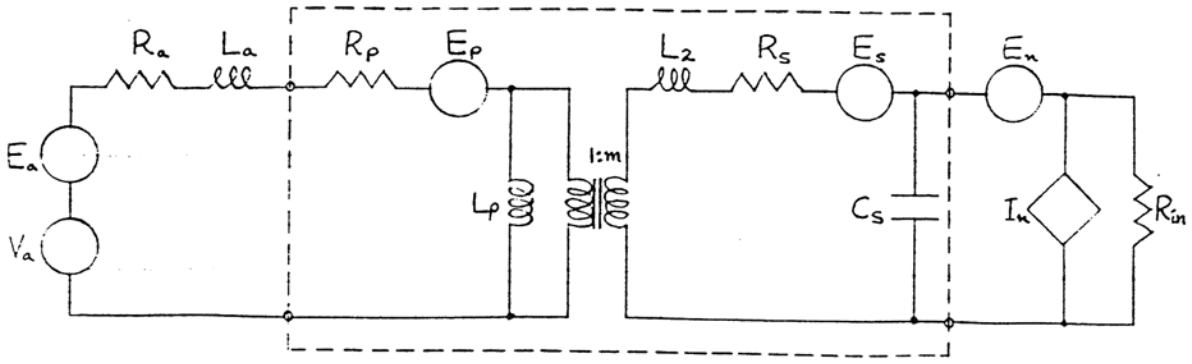

Figure 2.9. Input circuit: real transformer.

Figure 2.9 shows the equivalent input circuit of the VLF receiver with a realizable transformer. The transformer is modeled as an ideal transformer with a turns ratio of 1:m surrounded by various lumped elements which account for the actual behavior of the unit. R_p and R_s are the dc resistances of the primary and secondary windings, and E_p and E_s are the noise sources associated with these resistances. (We shall neglect resistance and noise due to core loss, as this is usually much smaller than winding loss. A coupling transformer is different from a power transformer where core loss is a major factor.) L_p represents the inductance of the primary (measured with the secondary open-circuited). L_2 is the leakage inductance referred to the secondary (the inductance measured at the secondary with the primary short-circuited). L_2 is due to incomplete coupling of the flux from the primary into the secondary. C_s is the equivalent shunt capacitance referred to the secondary.

2.8 Receiver Frequency Response: Real Transformer

The analysis of the input circuit with a real transformer is somewhat more complicated than with the ideal transformer in Section 2.4, but after some work we find

$$\frac{V_{in}}{V_a} = \frac{j\omega m L_p R_{in}}{\left\{ \begin{array}{r} [R_a + R_p + j\omega(L_a + L_p)][(R_s + j\omega L_2)(1 + j\omega C_s R_{in}) + R_{in}] \\ +j\omega L_p m^2 (R_a + R_p + j\omega L_a)(1 + j\omega C_s R_{in}) \end{array} \right\}}. \tag{2.26}$$

We can simplify this to get the approximate formula

$$\frac{V_{in}}{V_a} \simeq \frac{R_{in}}{j\omega m(L_a + pL_2/m^2)} \left[\frac{f}{f - jf_t}\right] \left[\frac{f}{f - jf_i}\right] \left[\frac{-jf_c}{f - jf_c}\right] \tag{2.27}$$

where

$$p = 1 + L_a/L_p \tag{2.28}$$

$$f_t = \frac{(R_a + R_p) \parallel (R_s + R_{in})p/m^2}{2\pi(L_a + L_p)} \tag{2.29}$$

$$f_i = \frac{R_a + R_p + (R_s + R_{in})p/m^2}{2\pi(L_a + pL_2/m^2)} \tag{2.30}$$

$$f_c = \frac{1}{2\pi C_s R_{in}}. \tag{2.31}$$

p is the reactive division ratio of the primary circuit. In an ideal transformer, L_p is infinite and we have $p = 1$. f_t is the frequency below which the shunting effect of L_p is important. f_i is the input turnover frequency (compare with Equation (2.15)). f_c is the high frequency rolloff associated with the shunting effect of C_s across R_{in}.

In a good design we require f_t to be much less than f_i. That is, the shunting effect of L_p must be small at the lowest frequency of interest. We also require f_c to be above the highest frequency of interest.

We can substitute the expression for V_a given in Equation (2.3) to find the amplifier input voltage as a function of the received wave, and we have

$$V_{in} = \frac{NAR_{in}B_w}{m(L_a + pL_2/m^2)} \left[\frac{f}{f - jf_t}\right] \left[\frac{f}{f - jf_i}\right] \left[\frac{-jf_c}{f - jf_c}\right]. \tag{2.32}$$

Equation (2.32) is illustrated in Figure 2.10.

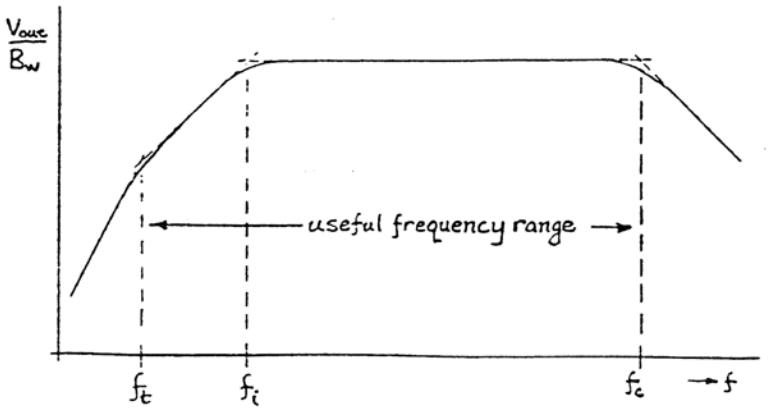

Figure 2.10. Relative frequency response.

Example: The Portable VLF Receiver has the following values:

$$\begin{aligned} p &= 1.122 \\ pL_2/m^2 &= 6.9\ \mu\text{Hy} \\ f_t &= 9.5\ \text{Hz} \\ f_i &= 349\ \text{Hz} \\ f_t &= 264\ \text{kHz}. \end{aligned}$$

Note that the effective leakage inductance in the primary circuit, pL_2/m^2, is negligible compared to the antenna inductance L_a (1 mHy). The major effect of L_2 is to raise the input impedance of the receiver as seen at the antenna terminals at high frequencies, an unimportant effect.

2.9 Receiver Noise Figure: Real Transformer

Referring to Figure 2.9, we can solve to find the noise at the amplifier input, and divide by the gain in Equation (2.26) to find the circuit niose referred to the source, E_{ni}. We find

$$E_{ni} \simeq E_a^2 + E_p^2 + \frac{E_s^2}{m^2}p^2\left(1+\frac{f_{tn}^2}{f^2}\right) + \frac{E_n^2}{m^2}\left[\left(p-\frac{f^2}{f_{cn}^2}\right)^2 + p^2\frac{f_{tn}^2}{f^2}\right] + I_n^2 m^2 R_a^2\left(1+\frac{f^2}{f_a^2}\right) \tag{2.33}$$

where

$$f_{tn} = \frac{R_a + R_p}{2\pi(L_a + L_p)} \tag{2.34}$$

and

$$f_{cn} = \frac{1}{2\pi(C_s m^2 L_a)^{1/2}}. \tag{2.35}$$

The noise factor is then given by

$$F = 1 + \frac{R_p}{R_a} + \frac{p^2 R_s}{m^2 R_a}\left(1+\frac{f_{tn}^2}{f^2}\right) + \frac{E_n^2}{4kTm^2R_a}\left[\left(p-\frac{f^2}{f_{cn}^2}\right)^2 + \frac{p^2 f_{tn}^2}{f^2}\right] + \frac{m^2 I_n^2 R_a}{4kT}\left(1+\frac{f^2}{f_a^2}\right). \tag{2.36}$$

We can make the following approximations at different frequencies:

1. At low frequencies,

$$F \simeq 1 + \frac{R_p}{R_a} + \left(\frac{R_s}{m^2 R_a} + \frac{E_n^2}{4kTm^2R_a}\right)p^2\left(1+\frac{f_{tn}^2}{f^2}\right). \tag{2.37}$$

2. At middle frequencies,

$$F \simeq \frac{m^2 I_n^2 R_a}{4kT}\cdot\frac{f^2}{f_a^2}. \tag{2.38}$$

3. At high frequencies,

$$F \simeq \frac{E_n^2}{4kTm^2R_a}\cdot\frac{f^4}{f_{cn}^4}. \tag{2.39}$$

Comparing these equations with Equation (2.24) we see that the input transformer has the following effects:

1. The low-frequency noise contribution of E_n is multiplied by the factor p. This is the most important low-frequency effect. For good noise performance we require that p be as small as possible, or that the primary inductance L_p be much greater than the antenna inductance L_a. In the Portable VLF Receiver we have $p = 1.122$, increasing the noise factor F by 0.259.

2. At frequencies below f_{tn}, the transformer coupling noise corner frequency, the noise figure deteriorates. We would like f_{tn} to be as low as possible. Note that f_{tn} is greater than f_t, the gain turnover frequency, and so the noise requirement is more stringent than the requirement for good frequency response. In the Portable VLF Receiver we have $f_{tn} = 18$ Hz.
3. The winding resistances R_p and R_s increase the low-frequency noise figure. The effect of R_s is multiplied by p. We must keep the winding resistances as small as possible. In the Portable VLF Receiver winding loss increases F by 0.088.
4. There is no appreciable effect at middle frequencies.
5. At frequencies above the shunt capacitance noise corner frequency f_{cn}, the noise figure deteriorates rapidly. As the reactance of C_s decreases, more of the voltage due to the amplifier noise source E_n appears across the input of the amplifier (this didn't happen in the ideal-transformer case). We require that f_{cn} be as high as possible. Again the requirement for good noise performance is more restrictive than that for good high-frequency response. In the Portable VLF Receiver we have $f_{cn} = 6.48$ kHz, and the effect of E_n dominates that of I_n above 20 kHz.

Summarizing the above effects, we see that for good noise performance L_p should be as large as possible, and R_p, R_s, and C_s should be as small as possible. Needless to say, these are conflicting requirements as far as transformer design goes. We can increase L_p by winding more turns of smaller wire on the transformer, but this will increase R_p and R_s, and may increase C_s as well. We shall consider this question in more detail in Chapter 4.

Example: Consider the Portable VLF Receiver with $m = 22.80$, and f_{tn} and f_{cn} as given above. Figure 2.11 shows the sensitivity of the receiver with the 56.7 cm loop antenna for both the ideal and real transformer cases. Especially note the deterioration above f_{cn} with the real transformer.

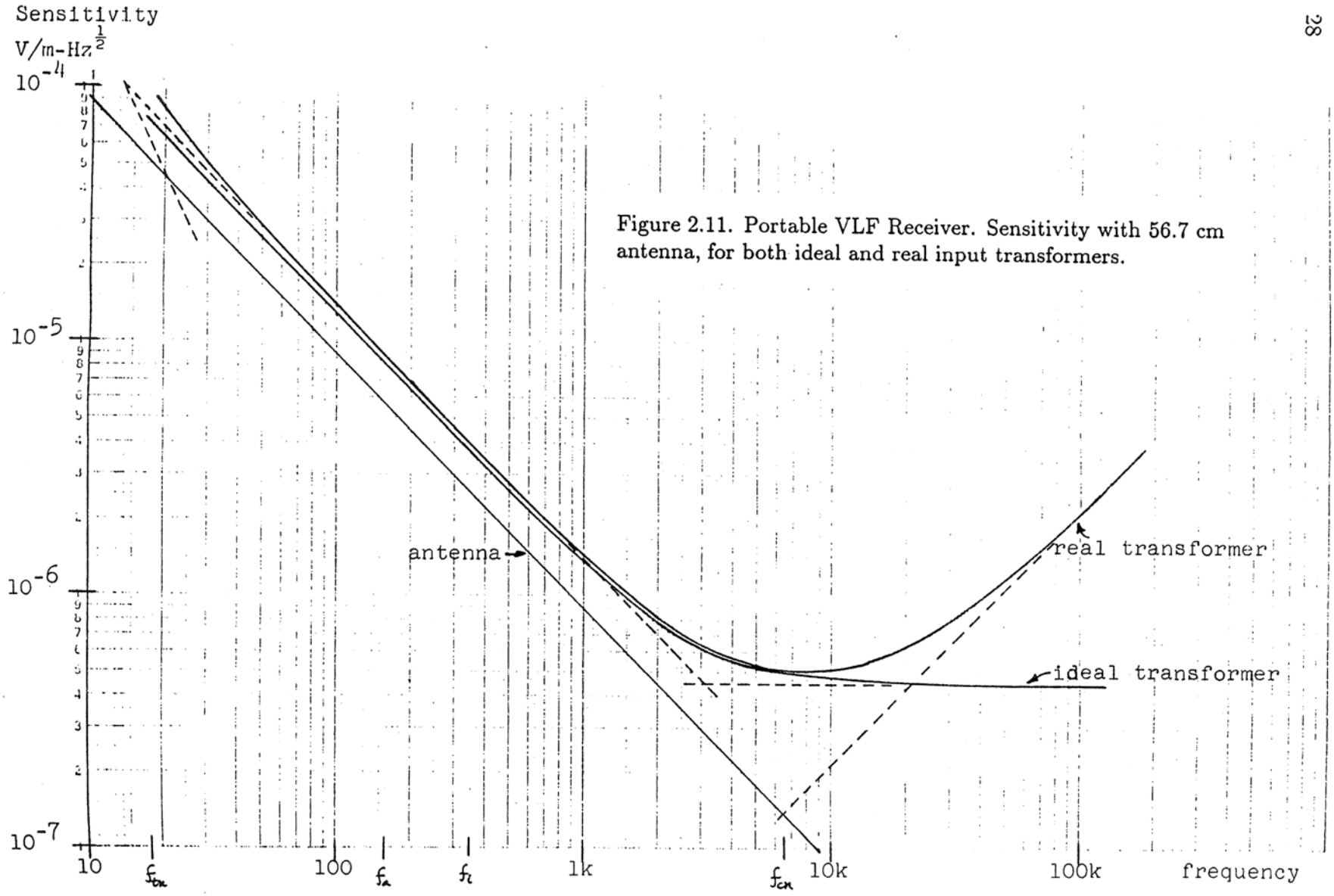

Figure 2.11. Portable VLF Receiver. Sensitivity with 56.7 cm antenna, for both ideal and real input transformers.

3. Loop Antenna Design

3.1 Loop Antenna Parameters

In this chapter we shall discuss the design of air-core loop antennas to fit particular receiving system requirements. Figure 3.1 shows the equivalent circuit of the antenna (omitting the negligible radiation resistance R_r), and Figure 3.2 shows the physical dimensions of the antenna.

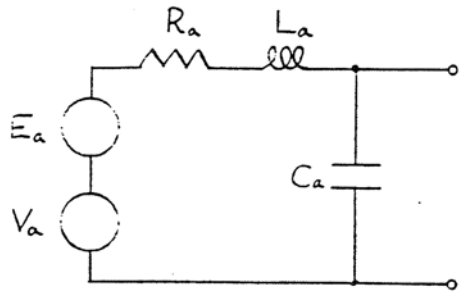

E_a = loop noise voltage
V_a = loop signal voltage
R_a = loop dc resistance
L_a = loop inductance
C_a = loop distributed capacitance

Figure 3.1. Loop equivalent circuit.

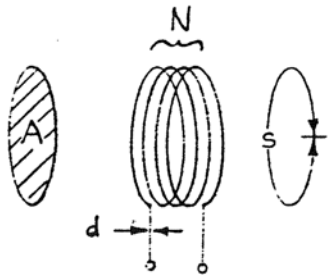

N = number of turns
A = area of each turn
d = diameter of wire
s = length of each turn

Figure 3.2. Loop physical dimensions.

We have shown the loop as a single-layer solenoid for clarity. In fact, for accuracy in the inductance calculations that follow, the turns must be tightly bundled together with as little space between wires as possible.

The designer can choose the wire size and material, the area and shape of the loop, and the number of turns in an effort to meet design specifications that include the antenna

impedance (R_a and L_a, or R_a and f_a) and normalized sensitivity S_0. There are some constraints on possible designs, of course. As we shall see, more sensitive loops (smaller S_0) are bigger and weigh more than less sensitive ones. Also, since we are restricted to using an integral number of turns and discrete wire sizes, finding an antenna of a particular impedance and sensitivity will involve a choice among several approximate designs.

In the following sections we shall give functions for the various design specifications in terms of the physical parameters, and then we shall develop a method to invert these functions to find the physical parameters given the specifications.

3.2 Resistance R_a

The dc resistance of the antenna (which determines the noise source E_a) is simply

$$R_a = \frac{4\rho N s}{\pi d^2} \qquad [\Omega] \tag{3.1}$$

where ρ is the resistivity of the wire. For copper (the usual choice) we have $\rho = 1.724 \times 10^{-8}$ Ω m. It is convenient to express the resistance in terms of the area of the loop A, rather than the length of each turn s. We can express s as

$$s = c_1\sqrt{A} \tag{3.2}$$

where c_1 is a constant that depends on the shape of the loop. For a circular loop, $c_1 = 2\sqrt{\pi}$; for a square loop, $c_1 = 4$. Table 3.1 lists the constant c_1 for a variety of loop shapes. We then have

$$R_a = \frac{4\rho N c_1\sqrt{A}}{\pi d^2} \qquad [\Omega]. \tag{3.3}$$

Note that we have only calculated the dc resistance. Because of the skin and proximity effects, the actual ac resistance at higher frequencies may be greater; but this has little practical effect in real loops.

3.3 Inductance L_a

The inductance can be expressed as

$$L_a = 2.00 \times 10^{-7} N^2 c_1 \sqrt{A} \left[\ln\left(\frac{c_1 \sqrt{A}}{\sqrt{N} d} \right) - c_2 \right] \quad \text{[Hy]}. \tag{3.4}$$

The formula gives L_a in henries when d and A are in meters and meters^2. $\ln(\cdot)$ is the natural logarithm function. The values of the constants c_1 and c_2, which depend on the shape of the loop, are given in Table 3.1. This formula is adapted from *Terman* [1943], Equation (2.35) (with low frequency correction), and uses the approximation $\sqrt{N}d$ for the diameter of the conducting bundle of wires in loops with more than one turn. There is a small error associated with this approximation (since a bundle of two wires does not have a circular cross-section), but for $N = 1$ or $N \geq 5$ the error, which over-estimates the actual inductance, is less than 2%. For Equation (3.4) to apply accurately, it is essential that the bundle of wires in the loop be as close together as possible, else the coupling between wires will not be as tight as assumed and the actual inductance will be lower. When constructing a multi-turn loop it is necessary to bind the wire bundle; lacing twine works well on all but the largest loops.*

Table 3.1. Numerical Constants c_1 and c_2

Shape of Loop	c_1	c_2
circular	3.545	0.815
regular octagon	3.641	0.925
regular hexagon	3.722	1.000
square	4.000	1.217
equilateral triangle	4.559	1.561
right isosceles triangle	4.828	1.696

* In fact, spacing turns to lower the turn-to-turn coupling can improve the system noise figure slightly at high frequencies by decreasing the inductance L_a for a given loop area A, though with some increase in construction difficulty. The design trade-offs are beyond the scope of the present discussion.

3.4 Turnover Frequency f_a

The antenna turnover frequency f_a is defined as the frequency where the loop reactance (due to L_a) equals the loop resistance. From Equation 2.1 we have

$$f_a = \frac{R_a}{2\pi L_a} \tag{2.1}$$

or

$$f_a = \frac{2\rho}{2 \times 10^{-7}\pi^2 N d^2 [\ln(c_1\sqrt{A}/\sqrt{N}d) - c_2]}. \tag{3.5}$$

Note that f_a depends only logarithmically (weakly) on A. Also, for a fixed choice of f_a and A, the bundle diameter $\sqrt{N}d$ is a constant.

3.5 Normalized Sensitivity S_0

The normalized antenna sensitivity S_0 is given by Equation (2.8) as

$$S_0 = \frac{(4kTR_a)^{1/2}}{2\pi NA} \quad [\text{T Hz}^{1/2}] \quad = \frac{c(4kTR_a)^{1/2}}{2\pi NA} \quad [\text{V Hz}^{1/2}\text{m}^{-1}]. \tag{2.8}$$

Substituting for R_a we have

$$S_0 = \frac{(4kT\rho c_1)^{1/2}}{\pi^{3/2}\sqrt{N}dA^{3/4}} \quad [\text{T Hz}^{1/2}]. \tag{3.6}$$

Note that for a fixed f_a we can solve Equation (3.5) for $\sqrt{N}d$ as a function of A, and substitute that function in Equation (3.6). Thus, for a fixed f_a the sensitivity S_0 depends only on the area A, and not explicitly on the number or turns or the wire size. In practice f_a is fixed in a given design by noise and frequency response considerations. Then to make a more sensitive system we must increase the size of the antenna; we cannot merely wind more wire onto the same size form.

We can calculate the mass of wire in the antenna, and we find

$$M = \frac{\pi\delta c_1\sqrt{A}Nd^2}{4} \tag{3.7}$$

where δ is the density of the wire. For copper, $\delta = 8.5 \times 10^3$ kg m^{-3}. Solving for $\sqrt{N}d$ and substituting in Equation (3.6) we find the interesting result

$$S_0 = \frac{(4kT\rho\delta)^{1/2}c_1}{2\pi(AM)^{1/2}} \quad [\text{T Hz}^{1/2}]. \tag{3.8}$$

This shows that the sensitivity of the antenna depends on the product AM of the antenna area and antenna mass. More sensitive antennas must be bigger, heavier, or both.

Refer to Figure 3.3 for a graph of antenna sensitivity as a function of NA and R_a, and to Figure 3.4 for a graph of sensitivity and mass as functions of f_a and A.

Figure 3.3. Normalized antenna sensitivity (V $Hz^{1/2}m^{-1}$) *vs.* NA and R_a.

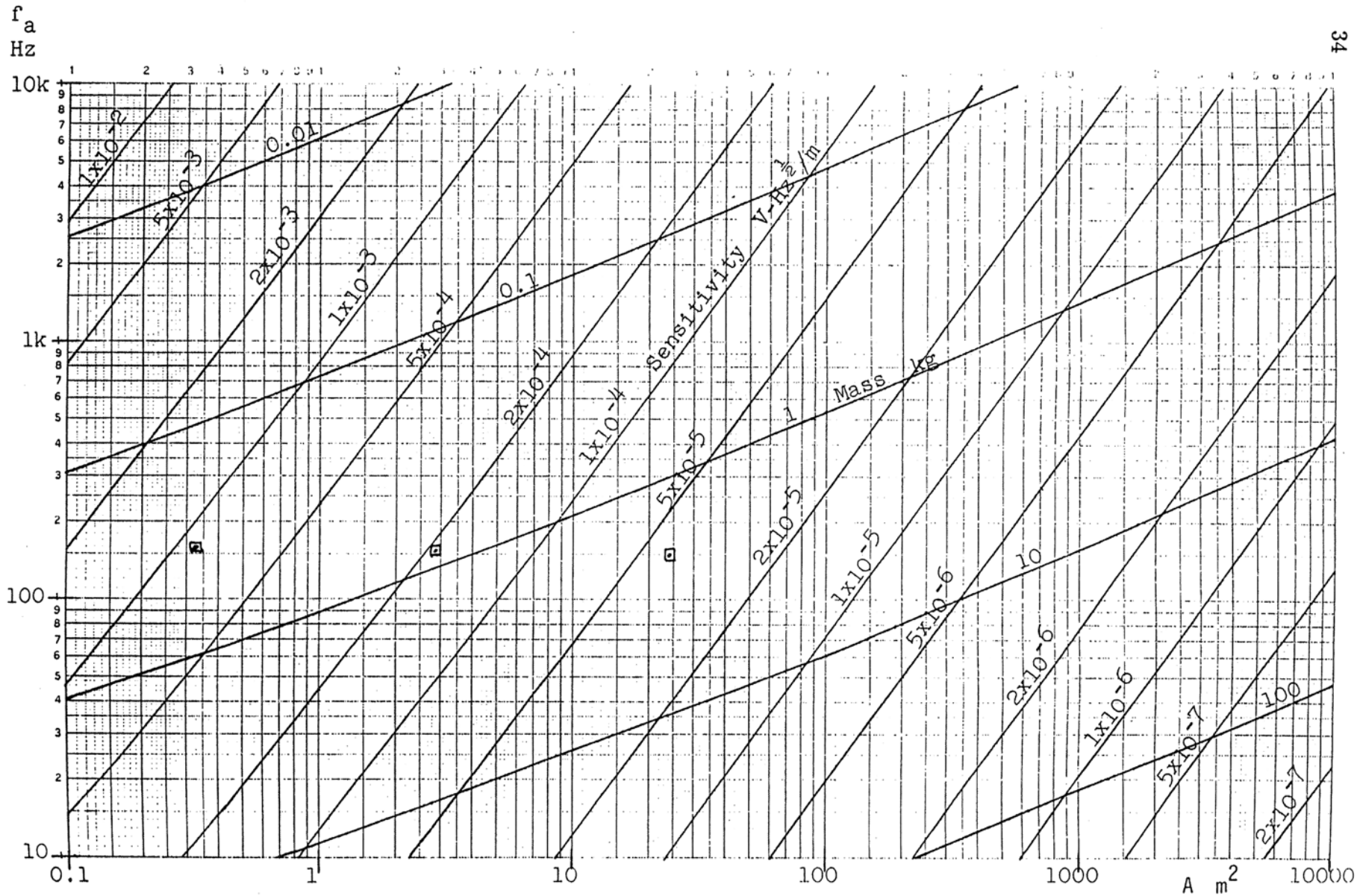

Figure 3.4. Normalized sensitivity and mass *vs.* A and f_a for square loop.

3.6 Distributed Capacitance and Resonance

Thus far we have ignored the effects of the distributed capacitance C_a of the loop. Unfortunately, it is difficult to calculate the value of C_a for practical loops, particularly where N is relatively small (say, less than 100 turns) and where successive turns may be randomly mixed in the bundle. It is easier to build a trial loop and measure its resonant frequency to find its capacitance. For example, the 56.7 cm standard loop for the Portable VLF Receiver has a resonant frequency around 180 kHz, giving a distributed capacitance of $C_a = 800$ pF.

Fortunately, the distributed capacitance is not as great a problem as it might seem at first glance. In a broad-band receiver with flat frequency response the input impedance of the receiver will be very low, on the order of R_a. This low load impedance on the antenna effectively shunts any effect of C_a. In any case, C_a is usually much less than $m^2 C_s$, the transformer capacitance referred to the primary, and can be ignored.

> *Example:* In the Portable VLF Receiver we have $m^2 C_s = 0.6$ μF, much larger than C_a (800 pF) for the 56.7 cm loop.

We can be sure that the distributed capacitance of the antenna will be as low as possible if we take care when winding the loop to separate turns of higher potential difference as far as possible. That is, the first and last turns should be on opposite sides of the bundle, with intermediate turns in between. Also, since distributed capacitance is only a weak function of the number of turns in an antenna of given size, we can minimize the effects of antenna capacitance by designing low-impedance antennas.

3.7 Antenna Design Algorithm

Now we present an algorithm for loop design. The design to meet specified R_a, L_a (or f_a), and S_0 is a matter of trial and error. Because we are restricted to using integral values of N and discrete wire sizes d, an exact solution is usually not possible. Because of the logarithmic dependence in Equations (3.4) and (3.5), these equations cannot easily be inverted. We are thus left with the task of making an estimate as to the correct values of A, N, and d, calculating the resulting impedance and sensitivity, and using the results to refine our estimate. The following procedure, implemented with the aid of a programmable calculator, seems to be the simplest. In the following, all dimensions are in meters and copper wire is used.

1. We are given R_a, L_a and f_a (see Equation (2.1)), and S_0.
2. Choose a shape for the loop and find c_1 and c_2 from Table 3.1
3. Choose an initial wire diameter d from Table 3.2, an initial number of turns N, and an initial area A. Refer to Figures 3.3 and 3.4 for help in estimating initial values. Begin the iterative procedure (Steps 4 through 7) with these values.

4. Call the value of area at this point A_i. Calculate the values of R_a and L_a (calling them R_i and L_i) for this area by the following formulae:

$$R_i = 2.195 \times 10^{-8} N c_1 \sqrt{A}/d^2 \qquad [\Omega], \tag{3.9}$$

$$L_i = 2.000 \times 10^{-7} N^2 c_1 \sqrt{A} \left[\ln(c_1\sqrt{A}/\sqrt{N}d) - c_2\right] \qquad [\text{Hy}]. \tag{3.10}$$

5. R_i and L_i are probably not the desired values. We shall find a new area A_{i+1} that gives the correct product $R_iL_i = R_aL_a$ by iteration. Note that A is proportional to this product. Choose A_{i+1} by the formula

$$A_{i+1} = \frac{R_aL_a}{R_iL_i} \cdot A_i. \tag{3.11}$$

Go to Step 4 and find new values R_{i+1} and L_{i+1} and repeat. This iteration will converge rapidly unless A becomes too small, in which case there is no solution. If that happens, choose a smaller N or d and try again.

6. Calculate f_a from

$$f_a = R_i/2\pi L_i. \tag{3.12}$$

If f_a is too high, increase N. If f_a is too low, decrease N. Go to Step 4. If $N = 1$ and f_a is still too low, there is no solution; choose a smaller wire size d and go to Step 4. We shall eventually find two solutions giving A and N for a given d that bracket the desired value of f_a. Choose the closest one.

7. Calculate the sensitivity from

$$S_0 = 2.02 \times 10^{-11} R_a^{1/2}/NA \qquad [\text{T Hz}^{1/2}] \tag{3.13}$$

or

$$S_0 = 6.05 \times 10^{-3} R_a^{1/2}/NA \qquad [\text{V Hz}^{1/2}\text{m}^{-1}].$$

If S_0 is too high (not sensitive enough), choose a larger wire size d. If S_0 is too small, choose a smaller wire size d. Go to Step 4. Eventually we shall find two solutions giving A, N, and d that have approximately the correct impedance and that bracket the desired value of S_0. Choose the one with the smaller S_0, thus making our antenna more sensitive than needed.

8. If desired, calculate the antenna mass (excluding insulation) from

$$M = 6.68 \times 10^3 c_1 \sqrt{A} N d^2 \qquad [\text{kg}]. \tag{3.14}$$

There are, of course, physical constraints on the antenna design. If the diameter of the wire bundle ($\sqrt{N}d$) is too large compared to the diameter of the loop it may be difficult to construct the antenna. Square loops, though they must be slightly larger than circular loops for the same sensitivity, are easier to build. Very large loops can be made triangular in shape, with the apex of the triangle supported by a tower (use insulators in the guy lines to the tower to be sure there are no closed current paths).

Table 3.2. Copper Wire Diameters

AWG Gauge	d [meters]	AWG Gauge	d [meters]
0	8.35×10^{-3}	20	8.12×10^{-4}
2	6.54	22	6.44
4	5.19	24	5.11
6	4.11	26	4.05
8	3.26	28	3.21
10	2.59×10^{-3}	30	2.55×10^{-4}
12	2.05	32	2.02
14	1.63	34	1.60
16	1.29	36	1.27
18	1.02	38	1.01
		40	7.99×10^{-5}

3.8 1 Ω/1 mHy Antennas for the Portable VLF Receiver

Table 3.3 shows the various antennas that can be used with the Portable VLF Receiver. These antennas were designed with the algorithm in Section 3.7 to have a nominal resistance of 1 Ω and inductance of 1 mHy, giving $f_a \approx 159$ Hz. They range from quite small portable antennas for local noise surveys to rather large antennas for high sensitivity.

Table 3.3. Antennas for the Portable VLF Receiver

Shape	Size, side or base	Wire AWG	N	R_a Ω	L_a mHy	f_a Hz	A m^2	S_0 V Hz$^{1/2}$m^{-1}	M kg
square	16.0 cm	20	47	1.002	0.998	159.8	0.02563	5.03×10^{-3}	0.132
	56.7 cm	18	21	1.006	0.994	160.9	0.3219	8.96×10^{-4}	0.331
	1.70 m	16	11	0.987	1.013	155.0	2.892	1.89×10^{-4}	0.831
	4.90 m	14	6	0.972	1.029	150.5	24.05	4.13×10^{-5}	2.09
right	2.60 m	16	12	0.994	1.005	157.5	1.695	2.97×10^{-4}	0.838
isosceles	8.39 m	14	6	1.004	0.996	160.3	17.59	5.74×10^{-5}	2.15
triangle	27.3 m	12	3	1.035	0.967	170.3	187.0	1.10×10^{-5}	5.56
	60.7 m	10	2	0.959	1.043	146.3	920.9	3.22×10^{-6}	13.1
	202 m	8	1	1.005	0.995	160.9	10164	5.97×10^{-7}	34.5

The right isosceles triangular loops are meant to be supported from a single mast at the apex of the triangle. The height of the loop is half the length of the base.

4. Input Transformer Design

4.1 Design Criteria

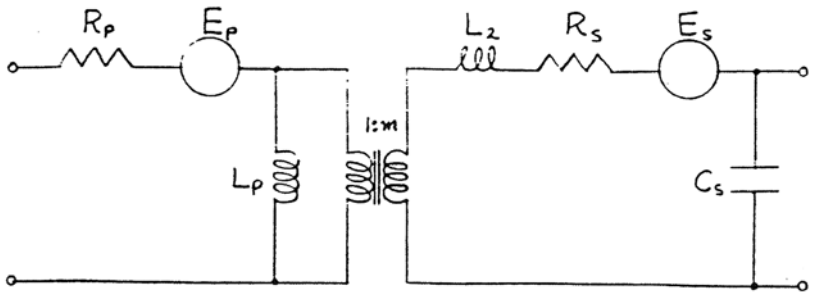

Figure 4.1. Transformer model.

Figure 4.1 shows the equivalent circuit of the input transformer (see Section 2.7). The transformer is modeled as an ideal transformer with turns ratio $1{:}m$ surrounded by various lumped elements. R_p and R_s are the winding resistances, L_p is the primary inductance, L_2 is the leakage inductance referred to the secondary, and C_s is the distributed capacitance referred to the secondary. Core loss is omitted.

The design of the input transformer proceeds from two requirements: frequency response and noise performance. Good frequency response requires that the transformer pass signals in the band of interest without significant attenuation. Good noise performance requires that the transformer decrease the receiver noise figure as little as possible. The noise requirement is generally more restrictive than the frequency response requirement. We shall discuss these two requirements as they apply to the values of each of the elements in Figure 4.1. We assume that the turns ratio m has already been chosen, perhaps by Equation (2.25). However, we might note that m does have a bearing on the realizable performance of the transformer—it is much more difficult to design a transformer that will give good wide-band performance if m is large (say, greater than 100) than if m is small.

1. L_p. For good frequency response, we require that f_t (Equation (2.29)) be below the lowest frequency of interest, or that the reactance of $L_a + L_p$ be large compared to the parallel resistance of R_a and R_{in}/m^2. For good noise performance, we require that f_{tn} be small (Equation (2.34)), or that the reactance of $L_a + L_p$ be large compared to R_a alone. Regardless of the lowest frequency of interest, we require that p (Equation (2.28)) be small for good low-frequency noise figure, or that L_p be much greater than L_a. This last requirement is usually the most restrictive.

2. R_p and R_s. The winding resistances are not usually important in terms of frequency response, but they may be significant in terms of noise performance. At frequencies above f_{tn} they increase the noise factor by the amount $(R_p + p^2 R_s/m^2)/R_a$ (Equation (2.36)). This is especially important at lower frequencies where the receiver noise figure is fairly low.
3. L_2. In most designs L_2 is relatively unimportant. Its major effect is to slightly raise the receiver input impedance at higher frequencies, an unimportant feature. The saving factor here is that L_2 appears in series with the antenna inductance as seen through the transformer, $m^2 L_a$, which is many times larger. Note that this is not the case when designing coupling transformers for resistive source and load, where leakage inductance often limits the highest usable frequency.
4. C_s. The effects of C_s appear at higher frequencies. For good frequency response f_c (Equation (2.31)) must be above the highest frequency of interest, or the reactance of C_s must be large compared to R_{in}. For good noise performance f_{cn} (Equation (2.35)) must be as high as possible. The sensitivity of the system deteriorates above f_{cn}, the resonant frequency of C_s and $m^2 L_a$. In practice, f_{cn} is less than f_c, and the noise requirement is more restrictive than that for frequency response. Minimizing C_s is a greater problem when the turns ratio m is large.

The general requirements above are to maximize L_p while minimizing R_p, R_s, and C_s. These are conflicting requirements, and a practical design involves a trade-off among them. For instance, with a given transformer core we can increase L_p by winding more turns on the primary and secondary. However, this increases R_p and R_s since we shall have longer wires in each winding, and may possibly have to use smaller diameter wire to boot. It may also increase C_s, though C_s is more affected by the method of winding than by the number of turns. Larger transformers usually give better performance over a given frequency range. A larger transformer will also required if the lowest frequency of interest is decreased.

4.2 Balancing and Shielding

So far we have assumed that the input transformer has a single primary and a single secondary winding. In actual fact the transformer should have a center-tapped primary, and in our design a center-tapped secondary as well. The center-tapped primary is necessary to balance the input circuit for common-mode signals from the antenna as might be caused by electrostatic pickup of precipitation static or radio frequency interference. A center-tapped secondary is an advantage in bipolar transistor designs because it allows us to use a differential input amplifier, desirable in terms of bias stability, common-mode rejection, and reduction of even-harmonic distortion. Also, bias currents flowing in the transformer secondary are balanced in a differential design, leaving no net dc field in the transformer core and making the unit less microphonic (vibration sensitive).

In order for the transformer to provide good common-mode rejection it is necessary that fields from each half of the primary be equally coupled into each half of the secondary. This can be achieved by bifilar (literally, "two-thread") winding. Two wires, representing each half of the primary or secondary are wound at once, for half the total number of turns, and the start of one wire is connected to the finish of the other to form the winding center-tap. Bifilar winding also ensures that each half of the winding has exactly the same number of turns. However, bifilar winding increases the distributed capacitance of the winding, especially in the secondary with its greater number of turns. This is not usually a problem in low-impedance design, but for high-impedance amplifiers where the turns ratio m must be large a different method must be used to balance the secondary windings. Because of the adverse effect on high-frequency noise figure due to C_s, bifilar winding may not be suitable even for low-impedance amplifiers above, say, 100 kHz.

Electrostatic coupling between the primary and secondary can cause problems by coupling HF signals directly into the amplifier where they may be demodulated and create interference. This can be reduced by an electrostatic shield between the windings. In the pot-core transformer discussed in the next section the secondary is shielded by wrapping a thin strip of metal around it before the primary is wound. In large metal-core transformers it may also be useful to have magnetic shielding around the outside of the transformer to attenuate pickup from stray magnetic fields. Pot-core transformers are inherently well-shielded for magnetic fields.

4.3 1 Ω:520 Ω Pot-Core Transformer Design for Portable VLF Receiver

The Portable VLF Receiver uses a pot-core input transformer—two ferrite cups clamped together around a bobbin on which are wound the transformer windings. A pot-core transformer was chosen over other possible designs (such as toroidal or E-I core transformers) because of its inherent good magnetic shielding and ease of fabrication. Designing a pot-core transformer involves two steps: selecting the core, and choosing the wire sizes and numbers of turns for the windings. There is a certain amount of cut-and-try involved in finding a good design.

The object of core selection is to find a core that will minimize the transformer contribution to the receiver noise figure by allowing a large primary inductance L_p but small winding resistances R_p and R_s. A measure of the suitability of a given core is the ratio L_p/R_p that it allows. The inductance L_p for a given core and winding is given by

$$L_p = \frac{\mu_0 \mu_r A_c N_p^2}{\ell_m} \tag{4.1}$$

where $\mu_0 = 4 \times 10^{-7}$ Hy m^{-1}, μ_r is the relative permeability of the core material, A_c is the effective core area, N_p is the number of turns in the primary, and ℓ_m is the effective magnetic path length. Pot-core manufacturers usually give this information in the form of the *inductance factor* A_L, where

$$L_p = A_L N_p^2. \tag{4.2}$$

A_L is usually given in units of nHy/turn^2 (or equivalently mHy @ 1000 turns).

The resistance R_p of the primary winding can be found from

$$R_p = \frac{\rho \ell_t N_p^2}{k W_a} \tag{4.3}$$

where ρ is the resistivity of the wire ($= 1.724 \times 10^{-8}$ Ω m for copper), ℓ_t is the average length per turn, W_a is the winding area of the bobbin, and k is a factor indicating how much of the bobbin area is actually primary conductor. In typical pot-core designs k ranges from 0.30 to 0.35.

Combining Equations (4.2) and (4.3) we see that the ratio of L_p to R_p is

$$\frac{L_p}{R_p} = \frac{k A_L W_a}{\rho \ell_t} = 2.0 \times 10^7 \frac{A_L W_a}{\ell_t} \qquad [\text{Hy } \Omega^{-1} = \text{s}]. \tag{4.4}$$

This figure of merit is a function of the pot-core specifications, but does not depend on the wire size or number of turns.

If we have chosen the transformer turns ratio m from Equation (2.25) so that $E_n^2/m^2 = 4kTR_a$ (giving a low-frequency noise figure of 3.01 dB with an ideal transformer), then the

low-frequency noise factor with a real transformer (Equation (2.37)) at frequencies above f_{tn} is

$$F \simeq 1 + \frac{R_p}{R_a} + \left(\frac{R_s}{m^2 R_a} + 1\right)\left(1 + \frac{L_a}{L_p}\right)^2. \tag{4.5}$$

If we use equal bobbin area for the primary and secondary windings, then $R_p = R_s/m^2$, and we can express Equation (4.5) as

$$F = 1 + \alpha + (1+\alpha)\left(1 + \frac{1}{\alpha\beta}\right)^2 \tag{4.6}$$

where

$$\alpha = R_p/R_a \tag{4.7}$$

and

$$\beta = 2\pi f_a L_p/R_p. \tag{4.8}$$

Note that β depends on the antenna turnover frequency f_a and on the core figure of merit L_p/R_p. For each value of β there is some value of α that minimizes the low-frequency noise figure. Figure 4.2 shows α and β as functions of the minimum obtainable noise figure. For instance, if we desired a transformer design that added no more than 1.00 dB to the ideal low-frequency noise figure (total $NF = 4.01$ dB), we find that the transformer should have a β of greater than 70, and $R_p = 0.13R_a$.

> *Example:* For the Portable VLF Receiver we have used a Magnetics, Inc. pot-core F43428-UG, with a single-section bobbin. This pot-core has $A_L = 7550 \times 10^{-9}$ Hy/turn^2, $W_a = 0.974$ cm^2, and $\ell_t = 0.220$ feet (an unfortunate mix of units), giving $L_p/R_p = 0.219$. With $f_a = 159.2$ Hz, we have $\beta = 219$. Thus we could hope to achieve a low-frequency noise figure of $NF = 3.58$ dB, using $R_p = \alpha R_a = 0.075\ \Omega$.

Figure 4.2 can be an aid to the selection of the transformer core, but the following points must be kept in mind:

1. Figure 4.2 applies only to the case $E_n/m = E_a$, with a best possible low-frequency $NF = 3$ dB. If the low-frequency noise figure is very important it is better to increase m and sacrifice some high-frequency performance than use an impractically large core.
2. It may be impossible to achieve packing densities as high as 0.35 for each winding, necessitating a larger core. This is a problem especially with the primary, which is likely to consist of a few turns of relatively large wire.
3. If good performance is desired much below f_a it will be necessary to use a larger L_p in order to keep f_{tn} and f_t below the lowest frequency of interest, necessitating a larger core.

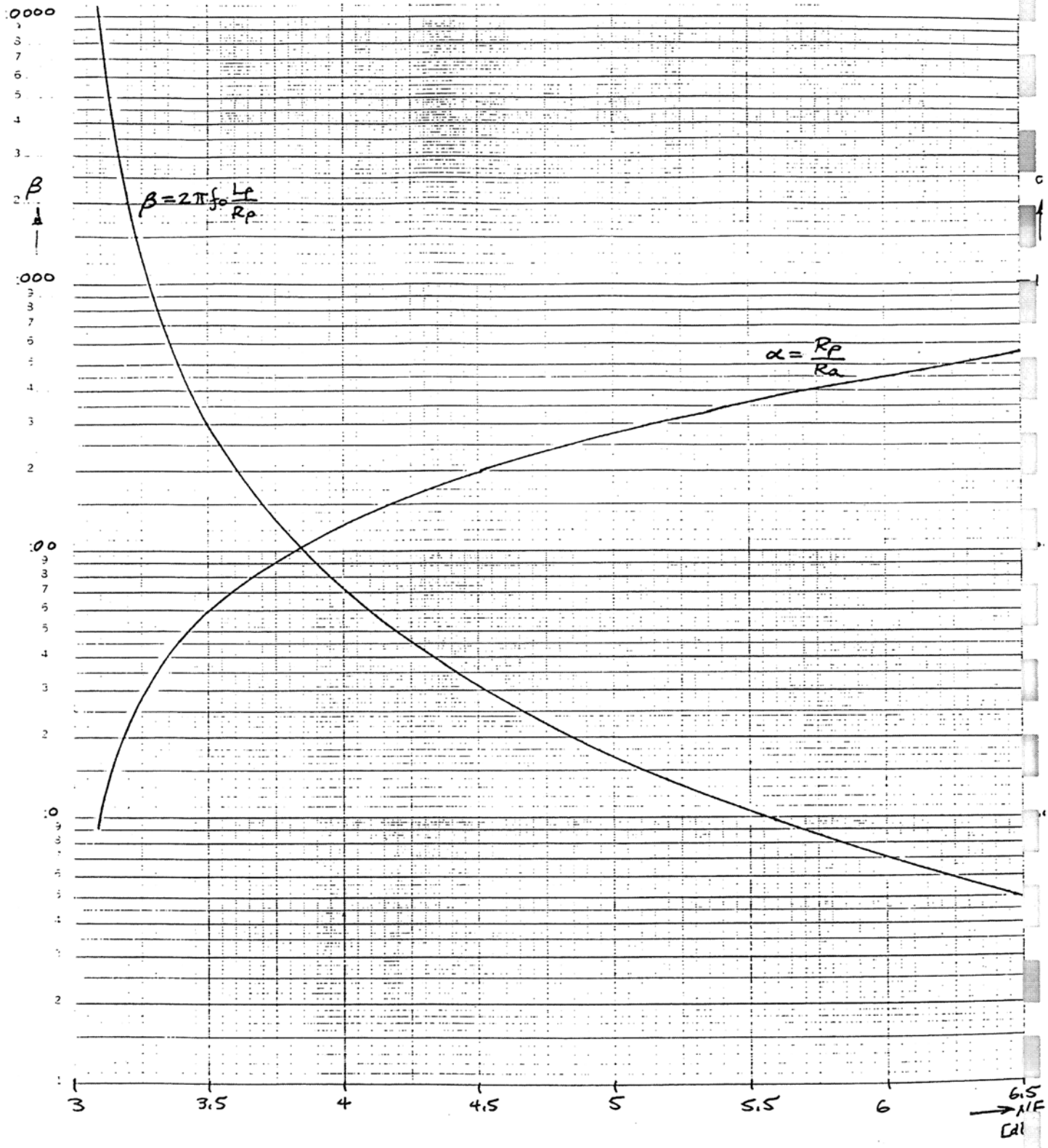

Figure 4.2. Transformer figure of merit and primary resistance ratio *vs.* achievable noise figure.

4. To keep C_s small for good high-frequency performance it may be necessary to separate successive layers in the secondary winding, which means using a larger core. With bifilar winding it is better to use fewer turns to reduce C_s, which means finding a core with a higher A_L value.
5. We have neglected core loss, which may increase the noise figure slightly.

Once the core has been selected, the next step is to calculate the wire sizes and numbers of turns required for each winding. In a transformer with an electrostatic shield we might use about 40% of the available bobbin area for each winding, leaving 20% for the shield and wrappings. From Figure 4.2 we can find the approximate values of L_p and R_p we hope to obtain, but it may be useful at this point to construct a table of L_p, R_p, and R_s for different choices of numbers of turns and wire sizes, and calculate NF from Equation (4.5) to find the optimum combination. Since N_p and N_s must be integers, and since wire comes in discrete sizes, there may not be a solution giving the exact value of NF from Figure 4.2.

It will probably be necessary to wind a few trial transformers and measure their values. Other factors enter at this point. For instance, if the core is small and the primary consists of a few turns of very large wire it may be difficult to wind; we may have to use a parallel combination of windings with smaller wire. Litz wire is ideal for this. If C_s is too large, a potential problem with bifilar winding, it may be necessary to compromise and use fewer turns than would be optimum at low frequencies.

When building the transformer, it is best to wind the secondary first, closest to the inside of the bobbin. This will decrease R_s slightly (since the average length of turn is less), compensating for the fact the E_s is magnified by p in the noise factor equation. Even more important, the smaller winding also minimizes C_s. After the secondary is wound and taped, the electrostatic shield can be wrapped over it (a wire must first be soldered to the shield to ground it external to the pot-core). Be sure that the ends of the shield do not touch each other (or are insulated) so the transformer will not have a shorted turn. Next the shield is taped and the primary is wound and taped. When the pot-core halves are assembled around the bobbin, be sure that their surfaces are clean so that they mate as closely as possible. Any space between them will decrease the inductance factor. This is especially a problem with very high permeability cores (such as Magnetics, Inc. "J" material). The cores may have to be glued together in larger sizes, but mounting clamps that work adequately are available for the smaller sizes. Once the transformer has been assembled and tested, the windings should be sealed and the bobbin fixed to the core to reduce microphonics. Polystyrene Q-dope painted into the pot-core openings will hold everything in place.

Schematic 9.3 shows the construction of the input transformer for the Portable VLF

Receiver. The transformer has the following values:

$$
\begin{aligned}
m &= 22.8 \\
L_p &= 8.2 \text{ mHy} \\
R_p &= 0.039\ \Omega \\
R_s &= 20.2\ \Omega \\
L_2 &= 3.2 \text{ mHy} \\
C_s &= 1160 \text{ pF}
\end{aligned}
$$

giving

$$
\begin{aligned}
NF &= 3.70 \text{ dB (at low frequencies)} \\
f_{tn} &= 18 \text{ Hz} \\
f_t &= 9.5 \text{ Hz} \\
f_{cn} &= 6.5 \text{ kHz} \\
f_c &= 264 \text{ kHz}
\end{aligned}
$$

Note that the low-frequency noise figure is larger than that predicted from Figure 4.2. We have had to reduce the number of turns in each winding in order to keep C_s to a tolerable value.

5. Input Amplifier Design

5.1 Amplifier Model

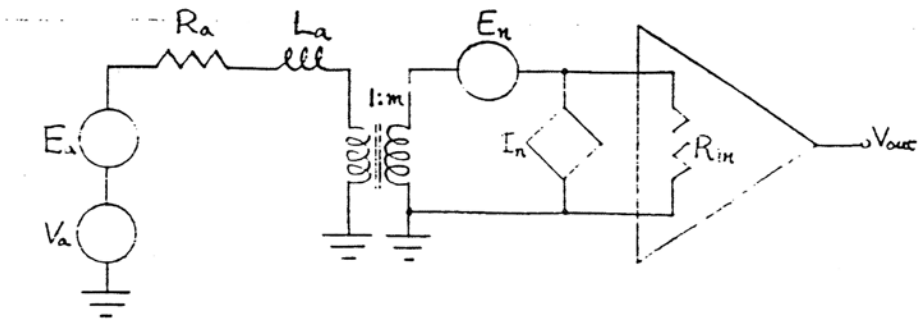

Figure 5.1. Receiver input equivalent circuit.

Figure 5.1 above shows the equivalent circuit of the input section of the VLF receiver. The amplifier is modeled as a noiseless amplifier preceded by noise voltage and noise current generators representing amplifier noise referred to the input. The antenna is connected to the amplifier by a transformer with turns ratio m. We shall assume that this is an ideal transformer. When designing the input amplifier we have two requirements in mind:

1. *Frequency Response.* For good low-frequency response we would like to keep the input turnover frequency f_i as low as possible. f_i is given by Equation (2.15) as

$$f_i = \frac{R_a + R_{in}/m^2}{2\pi L_a}. \tag{2.15}$$

   Above f_i the response of the receiver is independent of the frequency of the incident wave. Below f_i the output is proportional to frequency. We can use equalization to flatten the response below f_i, but because of considerations such as the dynamic range of the equalizer this sort of compensation is limited to a relatively narrow frequency range. Ideally we would make $R_{in}/m^2 = 0$, so we would have $f_i = f_a = R_a/2\pi L_a$, the lowest possible value. This is not practical, however. In the Portable VLF Receiver we have $R_{in}/m^2 \approx R_a$, giving $f_i \approx 2f_a$, a fair compromise.
2. *Noise Figure.* The noise factor F is given by Equation (2.23) as

$$F = 1 + \frac{E_n^2}{4kTm^2R_a} + \frac{I_n^2 m^2 R_a}{4kT}\left(1 + \frac{f^2}{f_a^2}\right) \tag{2.23}$$

$$\simeq 1 + \frac{E_n^2}{4kTm^2R_a} + \frac{I_n^2 m^2 R_a}{4kT} \cdot \frac{f^2}{f_a^2}. \tag{2.24}$$

We desire to keep the noise figure of the receiver as low as possible. As shown in Section 2.6, we can adjust the turns ratio m and trade off the noise figure at low frequencies against that at higher frequencies. A good choice is to set the low-frequency noise factor to be 2 ($NF = 3$ dB) by picking m to be (Equation (2.25))

$$m = E_n/(4kTR_a)^{1/2}. \tag{2.25}$$

Note that both the frequency response and the noise figure are affected by the choice of m. In most cases the noise figure requirement is more important and we choose m from Equation (2.25). Fortunately, in some amplifiers (such as the common-base circuit discussed below) this choice will also usually give $R_{in}/m^2 \leq R_a$ as desired for flat frequency response. However, the two requirements above *are* independent. As we shall see, some amplifier configurations are better able than others to meet both requirements.

5.2 Amplifier Figure of Merit

If we choose m by Equation (2.25) above, we can express the noise factor of the receiver as

$$F \simeq 2 + \frac{f^2}{(Mf_a)^2} \tag{5.1}$$

where

$$M = \frac{4kT}{E_n I_n} \tag{5.2}$$

The figure of merit M is a measure of the noise performance of the amplifier. The noise figure stays relatively low ($NF = 3$ dB) up to the frequency Mf_a, above which it deteriorates. In terms of system sensitivity, S falls with frequency up to Mf_a, where it levels off to a constant value (see Figure 2.7).

Example—Resistor as Input Termination. Consider using a resistor of value R_{in}, followed by a noiseless amplifier. This circuit can be modeled as in Figure 5.1 if we set $E_n = 0$, and $I_n = (4kTR_{in})^{1/2}$. In this case we find

$$F = 1 + \frac{m^2 R_a}{R_{in}}\left(1 + \frac{f^2}{f_a^2}\right). \tag{5.3}$$

For best noise performance we would make R_{in} infinite, but this makes f_i infinite also, giving the receiver a response proportional to frequency over all frequencies of interest. If we make $R_{in} = m^2 R_a$, setting $f_i = 2f_a$ with a low-frequency noise figure of $NF = 3$ dB, we find that

$$F = 2 + \frac{f^2}{f_a^2}. \tag{5.4}$$

Comparing this to Equation (5.1) we see that the resistor/noiseless amplifier combination has a noise figure of merit of only $M = 1$. Although it may seem surprising, we can do much better than this. The input impedance of an amplifier has no direct connection to the values of its equivalent input noise generators. *A well-designed amplifier with input resistance R can have input noise much smaller than the noise associated with an actual resistor of R ohms.* I stress this point because some researchers have made VLF receivers with resistor-terminated amplifier inputs, giving much poorer noise performance than might have been the case.

The noise performance of the amplifier can be no better than that of the active devices (transistors, op-amps, *etc.*) used in it. Figure 5.2 shows the values of E_n, I_n, and M for various bipolar and field-effect transistors, and operational amplifiers. It also shows the values of $E_n^2/4kT$ for these devices—that is, the source resistance m^2R_a to use for a low-frequency noise figure of $NF = 3$ dB. (These data have been culled from various manufacturers data sheets, and especially from *Motchenbacher and Fitchen* [1973]).

We see that there are some devices, particularly field-effect transistors, with very good noise performance. Bipolar transistors as a class are worse, though some still have respectable figures of merit. Op-amps are worse yet, with one being a negative performer compared to a simple resistor ($M < 1$).

Besides the noise figure of merit, we are also concerned with the input impedance of the amplifier. We would like to use an amplifier with a relatively low input impedance so that the input turnover frequency f_i is low, to give us flat frequency response to low frequencies. Our choices here are to either use a circuit with an inherently low input impedance, or use a high-impedance amplifier with feedback. We shall consider the latter case first.

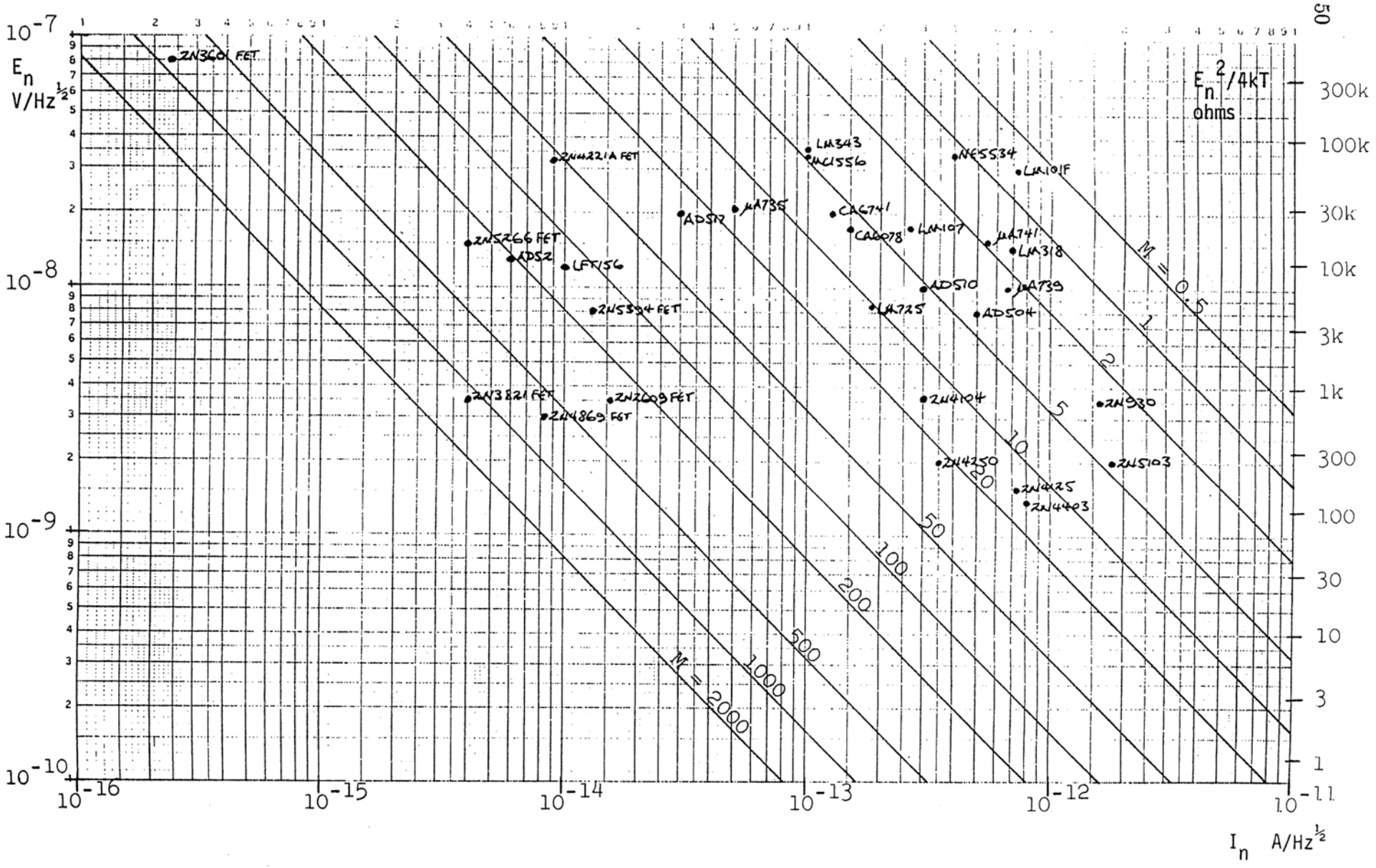

Figure 5.2. Active device noise figure of merit M, and noise generator E_n and I_n, at 1 kHz. Bipolar transistors measured

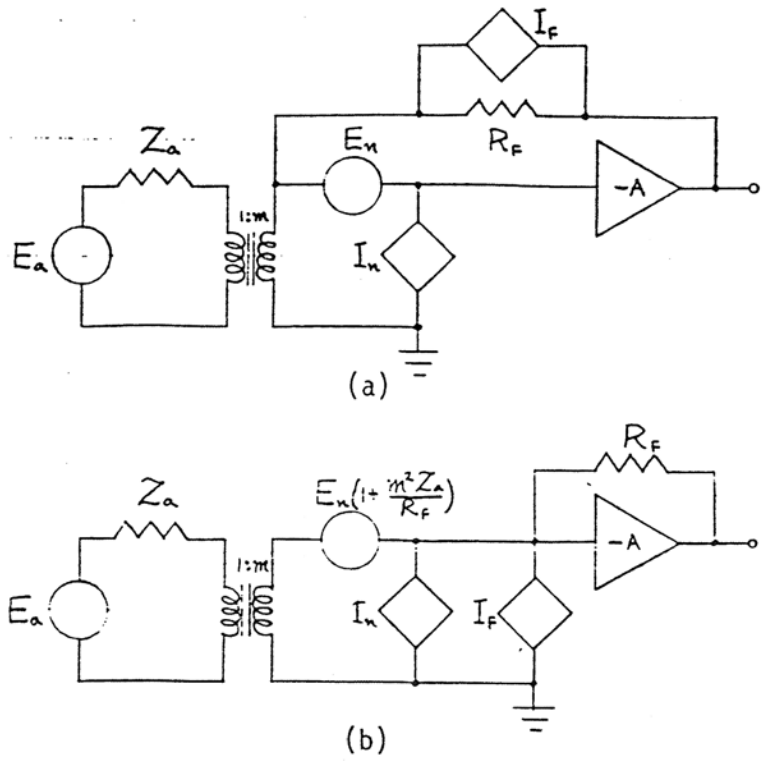

Figure 5.3. Amplifier with current feedback.

5.3 High-Impedance Amplifiers

Transistors in the common-emitter or common-source configuration and operational amplifiers have input impedances ranging from tens of kilohms on up. In order to use a circuit of this type it is necessary to employ negative current feedback at the input to lower and stabilize the input impedance of the amplifier. (As we saw above, merely shunting the input with a resistor ruins the noise figure.) However, there are limitations to this approach in terms of the realizable noise performance and stability of the circuit.

Figure 5.3 shows noise equivalent circuits of a high-impedance inverting amplifier with negative current feedback. The feedback resistor R_F has an equivalent noise current generator of $I_F = (4kT/R_F)^{1/2}$. In Figure 5.3(b) the noise sources have been referred to the input of the amplifier, ahead of the resistor R_f. The open-circuit voltage gain of the amplifier is $-A$. The input resistance of the amplifier with feedback is

$$R_{in} = \frac{R_F}{1+A} \tag{5.5}$$

and the noise factor is

$$F = 1 + \frac{E_n^2}{4kTm^2R_a}\left(1 + \frac{2m^2R_a}{R_F}\right) + \left(\frac{E_n^2}{R_F^2} + I_n^2 + \frac{4kT}{R_F}\right)\frac{m^2R_a}{4kT}\left(1 + \frac{f^2}{f_a^2}\right). \tag{5.6}$$

If we choose m so that $E_n^2 = 4kTm^2R_a$ (giving a low-frequency $NF \simeq 3$ dB), set R_f so that $R_{in} = m^2R_a$ (giving $f_i = 2f_a$), and assume that I_n^2 is negligible compared to $4kT/R_F$, we can approximate F as

$$F \simeq 2 + \left(\frac{1}{(1+A)^2} + \frac{1}{1+A}\right)\frac{f^2}{f_a^2} \tag{5.7}$$

and we see that the noise figure of merit M is

$$M < \sqrt{1+A}. \tag{5.8}$$

If the amplifier gain A is large enough the noise performance of the amplifier may be good, but the circuit may be very difficult to build.

> *Example:* Consider an amplifier with a gain of $A = 1000$, using a 2N3821 FET. From Figure 5.2 we find $E_n = 3.5 \times 10^{-9}$ V Hz$^{-1/2}$ and $I_n = 4 \times 10^{-15}$ A Hz$^{-1/2}$. Assuming $R_a = 1\ \Omega$, we choose $m = 27.6$ for a 3 dB low-frequency noise figure, and $R_F = 762\ \text{k}\Omega$ to give $R_{in} = 1\ \Omega$. The amplifier will have a figure of merit $M \simeq 32$; good but not outstanding. Note that the 2N3821 transistor without feedback has a figure of merit greater than 1000. For better performance with feedback we must have even higher amplifier gain. And unless the gain is well-defined and stable, we might want to use a smaller value of R_F to decrease R_{in} and stabilize the value of f_i (Equation (2.15)). For instance, if we chose $R_F = 76.2\ \text{k}\Omega$ giving $R_{in} = 0.1m^2R_a$, the figure of merit M decreases to less than 10.

While high-impedance amplifiers with feedback might give reasonably good noise performance if their gain and feedback resistor can be made high enough, the problem of circuit stability generally precludes their use. The input transformer shunt capacitance C_s forms a tuned circuit at the input of the amplifier with the transformed antenna inductance and leakage inductance. Any phase shift in the amplifier will cause the circuit to oscillate. We might use a lower-gain amplifier and build a stable circuit, but then the noise performance deteriorates. The low-impedance amplifiers discussed next are a much better practical solution.

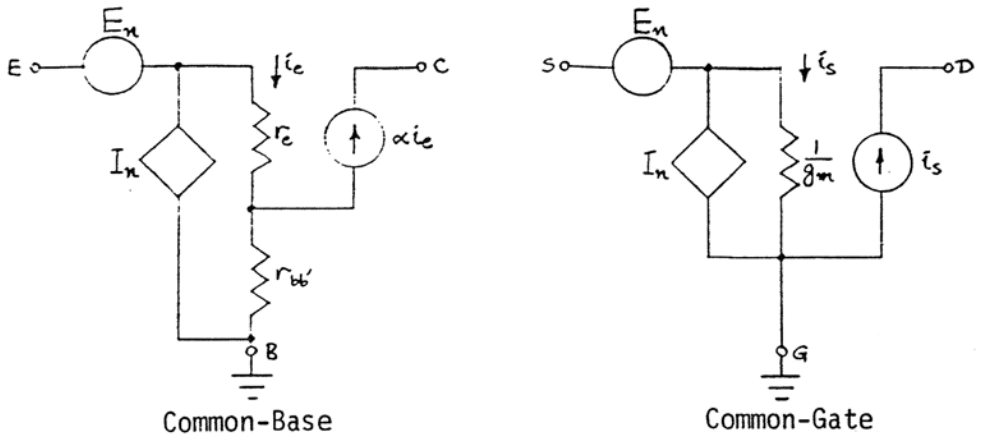

Figure 5.4. Low-impedance configurations.

5.4 Low-Impedance Amplifiers

There are two inherently low-impedance amplifier configurations of interest: the bipolar common-base circuit, and the field-effect transistor common-gate circuit. Figure 5.4 shows simplified equivalent circuits for these configurations. Note that the noise generators E_n and I_n in these circuits have the same values as when the transistors are used in the more usual common-emitter and common-source configurations.

From semiconductor theory we have the following:

1. Common-base amplifier:

$$E_n^2 = 4kTr_{bb'} + 2kTr_e \tag{5.9}$$

$$I_n^2 = 2qI_B = 2kT/\beta r_e \tag{5.10}$$

$$r_e = \frac{kT}{qI_E} = \frac{26\text{ mV}}{I_E} \tag{5.11}$$

$$R_{in} = r_e + r_{bb'}/\beta \simeq r_e \tag{5.12}$$

2. Common-gate amplifier:

$$E_n^2 \simeq 4kT/g_m \tag{5.13}$$

$$I_n^2 = 2qI_{GSS} \tag{5.14}$$

$$R_{in} = 1/g_m \tag{5.15}$$

where $q = 1.60 \times 10^{-19}$ coulomb. Note that noise sources E_n and I_n of real devices are always higher than the theoretical values given above, but these values are a starting point for discussion and represent the best performance we might be able to find.

For the bipolar transistor common-base circuit we want a transistor with a low intrinsic base resistance $r_{bb'}$ and high base-collector current gain β $(= h_{fe})$. If $r_{bb'}$ is small, the theoretical noise figure of merit for the bipolar transistor is

$$M = 2\sqrt{\beta}. \tag{5.16}$$

Note that $R_{in} \simeq r_e$ depends on the dc emitter current I_E. This can be controlled precisely in an actual circuit, so R_{in} is well-defined. Best noise performance is usually found with emitter currents in the range $I_E = 10$ to 100 μA, giving $R_{in} \simeq 260$ to 2600 Ω.

In the FET common-gate circuit, I_{GSS} can be extremely small, leading to very low values of I_n. E_n tends to be somewhat higher than suggested by Equation (5.13). Even so, FET's can have better noise figures of merit than bipolar transistors (see Figure 5.2). The transconductance g_m ranges from 500 to 5000 μS for typical low-noise FET's, giving $R_{in} \simeq 200$ to 2000 Ω. g_m depends slightly on the operating point (drain current), but more significantly both g_m and I_{DSS} (the zero-bias drain current) may vary over a 5 to 1 range among different units of a given transistor type. It may be necessary to select units for g_m (or I_{DSS}) to be sure that R_{in} and f_i have the desired values.

Another approach to overcome the variation in R_{in} with the common-gate circuit would be to lower the turns ratio m, thus decreasing R_{in} with respect to $m^2 R_a$, and stabilizing f_i. This will increase the noise figure at middle frequencies due to I_n. Unfortunately, in a real circuit (see Section 5.5 below) I_n of the amplifier is larger than the I_n of the input device alone, and this approach isn't very useful. In fact, as we shall see in Section 5.5, it is difficult to build a real amplifier that can take advantage of the extremely low current noise I_n of FET's in the common-gate configuration. In practical low input impedance circuits thay are really not much better than bipolar transistors in terms of their noise performance, though they may have other advantages, such as larger signal-handling ability.

The theoretical values for E_n and I_n listed above are just that—minimum values based on an understanding of the noise mechanisms in ideal devices. In practice transistors must be selected by referring to published values of E_n and I_n, or by independent testing in the laboratory. Also important, but not mentioned above, are the changes in E_n and I_n with frequency. At very low frequencies (depending on device type) all units experience $1/f$ noise due to surface defects. This can cause E_n in FET's, and both I_n and (to a lesser extent) E_n in bipolar's, to increase at low frequencies. Some devices are better in this respect than others. Unfortunately, manufacturer's data sheets do not often give noise generator values *vs.* frequency, if they give any values at all. At high frequencies capacitive

coupling in both types of transistors causes I_n to increase, but this effect is not usually important at frequencies below about 100 kHz. Again, only the data sheets or testing can tell.

To summarize, either bipolar transistors in the common-base configuration or field-effect transistors in the common-gate configuration are suitable for VLF receiver input amplifiers because of their low input impedances (a few hundred ohms) and good noise performance. FET's promise better noise figures, but these cannot be achieved in practice, making FET circuits only marginally better than bipolar circuits. Device types must be selected on the basis of published or measured values of E_n and I_n, as actual noise performance may be worse than theoretical models indicate. At the low-frequency end (say, below 1 kHz) $1/f$ noise may be important with some device types.

5.5 Low-Impedance Amplifier: Second Stage Noise

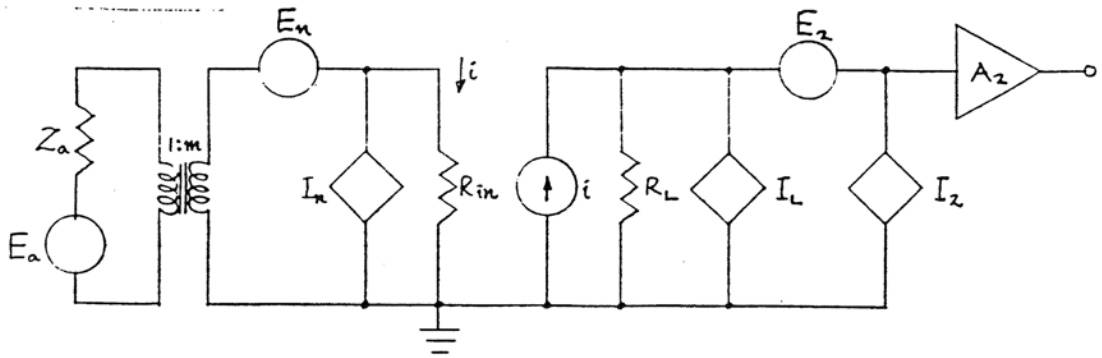

Figure 5.5. Low-impedance amplifier with second stage.

Figure 5.5 shows the ac equivalent circuit of a VLF receiver with a low-impedance input stage (either common-base or common-gate) followed by a second stage of amplification. R_L is the effective load of the first stage, the parallel combination of any load resistor and the output impedance of the first transistor, and I_L is the noise current of this resistance. E_2 and I_2 are the input noise sources for the second stage. Analyzing this circuit we find its noise factor as

$$\begin{aligned} F &= 1 + \frac{E_n^2}{4kTm^2R_a} + \frac{I_n^2 m^2 R_a}{4kT}\left(1 + \frac{f^2}{f_a^2}\right) \\ &\quad + \frac{|R_{in} + m^2R_a(1 + jf/f_a)|^2}{4kTm^2R_a}\left(I_L^2 + I_2^2 + \frac{E_2^2}{R_L^2}\right) \\ &\simeq 1 + \frac{E_n^2}{4kTm^2R_a} + \left(\frac{(I_n^2 + I_2^2)m^2R_a}{4kT} + \frac{m^2R_a}{R_L}\right)\frac{f^2}{f_a^2} \end{aligned} \qquad 5.17$$

where

$$I_L^2 = 4kT/R_L. \tag{5.18}$$

Note that I_L^2 and I_2^2 add directly to I_n^2. They may be much larger than I_n if the input stage is an FET. These current sources appear effectively at the input of the first stage, parallel to I_n, because the current gain of the input stage is close to unity. Or thinking of it another way, even though the first stage provides substantial voltage gain, its output impedance is so high that second-stage current noise is very important. We must keep I_2 small compared to I_n and use a large R_L in order to preserve the high-frequency noise figure of the input stage. If an input common-base stage is followed by a second bipolar stage, we should operate the second stage at a lower quiescent current to keep I_2 small. (The second stage might be a common-emitter or emitter-follower stage with $I_{E2} = 0.3I_{E1}$, for instance.)

Since the gain of the first stage depends on the parallel combination of the first transistor output impedance and R_L, the gain might vary with different transistor units, especially if R_L is very high. We may want to stabilize the circuit gain by using feedback as shown in Figure 5.6 below.

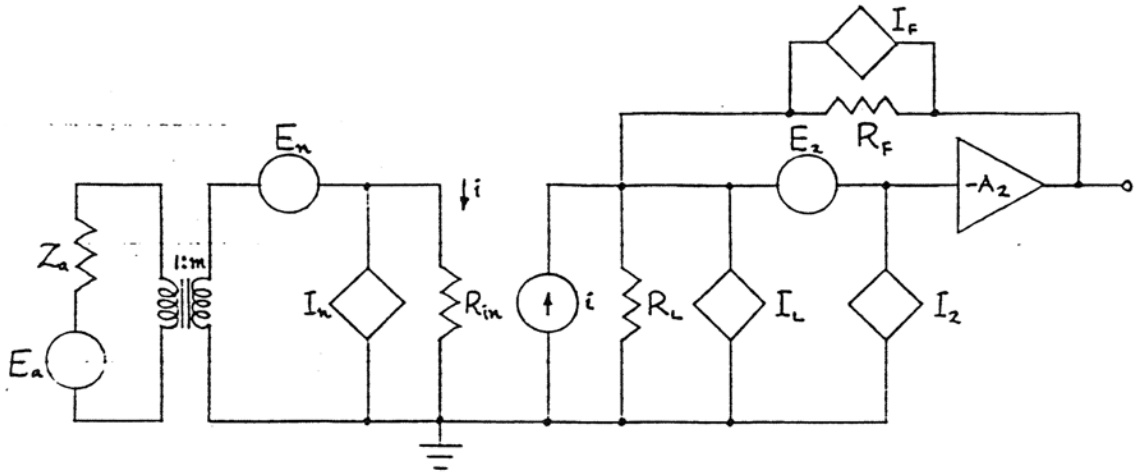

Figure 5.6. Low-impedance amplifier, second stage feedback.

Here we have used the resistor R_F around the second stage to decrease its input impedance. The gain of the circuit is now proportional to R_F, but relatively independent of R_L. In this case the noise factor is approximately

$$F \simeq 1 + \frac{E_n^2}{4kTm^2R_a} + \left(\frac{(I_n^2 + I_2^2)m^2R_a}{4kT} + \frac{m^2R_a}{R_L} + \frac{m^2R_a}{R_F}\right)\frac{f^2}{f_a^2}. \tag{5.19}$$

Now all three noise current generators I_L, I_2, and I_F appear in parallel with I_n at the input.

With careful design we can build a high-gain amplifier with noise performance not much worse than that of a common-base input stage alone. However, it is difficult in practice to make R_L and R_F large enough to take advantage of the low input current noise of a common-gate FET input stage. Thus we cannot realize the superior low-noise performance of FET common-gate circuits, and they become in practice not much better than bipolar input circuits.

5.6 Differential Low-Impedance Amplifiers

Figure 5.7(a) shows a VLF antenna connected through an input transformer with a turns ratio m' and a center-tapped secondary to two input amplifiers followed by a differential amplifier. In Figure 5.7(b) we have combined the various amplifiers into one differential amplifier. The output of this amplifier depends only on the difference in voltage at its two input terminals, and not on their sum (or common-mode voltage). In Figure 5.7(c) we have combined the various noise generators. We assume that each of the pairs of generators E_{n1}, E_{n2} and I_{n1}, I_{n2} have equal noise outputs, but are statistically independent.

Since the amplifier responds only to the differential voltage at its input, any current flowing through point A in Figure 5.7(b) (which would produce only a common-mode voltage) is unimportant, and we can cut the circuit at this point. Thus the two voltage generators E_{n1} and E_{n2} are effectively in series for differential signals, and we have

$$E_{n'}^2 = E_{n1}^2 + E_{n2}^2 \equiv 2E_n^2$$

or

$$E_{n'} = \sqrt{2}E_n. \tag{5.20}$$

Similarly, any current from the noise current generators I_{n1} and I_{n2} flowing through point B in Figure 5.7(b) will generate a common-mode voltage at the amplifier and can be ignored. Since I_{n1} and I_{n2} are statistically independent, half of their noise power will be differential and half will be common-mode (through point B). We thus have

$$I_{n'}^2 = \frac{I_{n1}^2}{2} = \frac{I_{n2}^2}{2} \equiv \frac{I_n^2}{2}$$

or

$$I_{n'} = I_n/\sqrt{2}. \tag{5.21}$$

The input resistance of the circuit is clearly the sum of the resistances of the two amplifiers, so

$$R_{in'} = 2R_{in}. \tag{5.22}$$

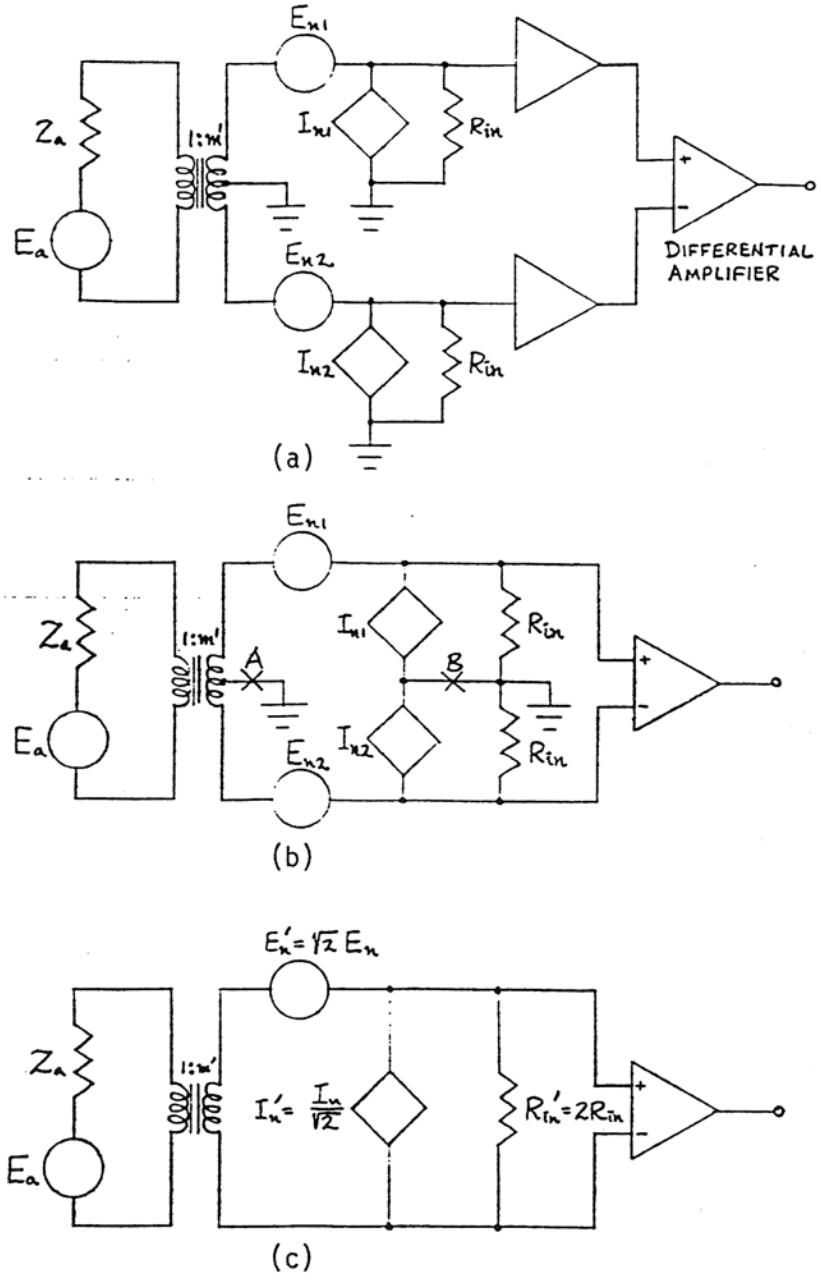

Figure 5.7. Differential input amplifier.

The noise factor of the differential circuit is

$$F = 1 + \frac{E_{n'}^2}{4kTm'^2R_a} + \frac{I_{n'}^2 m'^2 R_a}{4kT}\left(1 + \frac{f^2}{f_a^2}\right)$$
$$= 1 + \frac{2E_n^2}{4kTm'^2R_a} + \frac{I_n^2 m'^2 R_a/2}{4kT}\left(1 + \frac{f^2}{f_a^2}\right) \qquad 5.23$$

We can obtain noise performance identical to that of a single-ended input amplifier as in Equation (2.23) if we choose

$$m' = \sqrt{2}m \qquad (5.24)$$

where m is the corresponding turns ratio for the single-ended receiver.

We see that there is no difference in noise performance between a single-ended and a differential input amplifier. The frequency response is the same, also. The differential configuration does have several advantages, however. First, the differential amplifier will give better common-mode rejection, particularly if the input transformer uses bifilar winding in the secondary. Second, dc currents in the transformer secondary are balanced, making the transformer less microphonic. (With a single-ended input, quiescent emitter/source current creates a dc magnetic field in the transformer core. Any vibration will generate signals in the secondary.) Third, it may be easier to build a differential amplifier whose operating point is stable with temperature changes (improved bias stability). And last, any even-harmonic distortion in the input stages cancels. (Odd-harmonic distortion is unaffected.)

In order to retain the good noise figure of the single-ended input circuit, we must be sure that the differential amplifier following the input stages in the differential circuit has good common-mode rejection. If it does not, common-mode noise from the input stages will also be amplified, and the noise figure will be worse than anticipated. This is not usually a severe problem

> *Example:* In the Portable VLF Receiver, common-mode noise (which appears at the input of the receiver as an additional current noise generator) increases I_n by about 7%, or 0.6 dB.

6. Receiver Calibration

6.1 Induced *versus* Injected Calibration

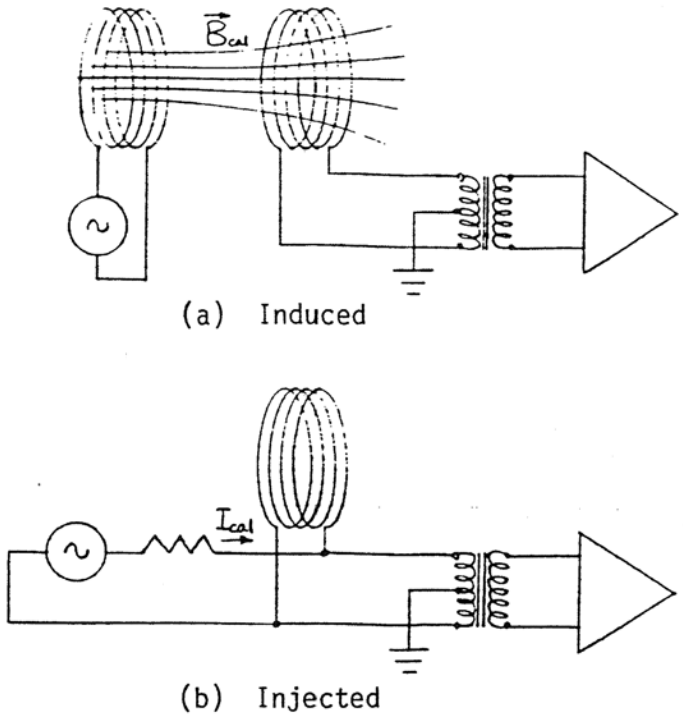

Figure 6.1. Receiver calibration methods.

In order to make accurate measurements of the strength of received signals it is necessary to determine the response of the VLF receiver to known fields. There are two common ways of doing this. The first method, which is illustrated in Figure 6.1(a), uses a separate calibration coil to generate a known magnetic flux through the VLF antenna. The second method, shown in Figure 6.1(b), uses a signal generator to inject a known current into the VLF receiver input in parallel with the antenna. Other possible injection methods use an additional transformer winding for current injection, or a separate transformer in series with the antenna to insert a known emf into the antenna circuit, but they are all similar.

The induced calibration method would appear to be superior, since we are inducing a signal in the antenna just as if an incident wave were being received, whereas the injected calibration method inserts the signal after the antenna. In fact, they are equally accurate and effective. It is usually impractical to separate the calibration coil far enough from the

The noise factor of the differential circuit is

$$F = 1 + \frac{E_{n'}^2}{4kTm'^2R_a} + \frac{I_{n'}^2 m'^2 R_a}{4kT}\left(1 + \frac{f^2}{f_a^2}\right)$$
$$= 1 + \frac{2E_n^2}{4kTm'^2R_a} + \frac{I_n^2 m'^2 R_a/2}{4kT}\left(1 + \frac{f^2}{f_a^2}\right) \qquad 5.23$$

We can obtain noise performance identical to that of a single-ended input amplifier as in Equation (2.23) if we choose

$$m' = \sqrt{2}m \qquad (5.24)$$

where m is the corresponding turns ratio for the single-ended receiver.

We see that there is no difference in noise performance between a single-ended and a differential input amplifier. The frequency response is the same, also. The differential configuration does have several advantages, however. First, the differential amplifier will give better common-mode rejection, particularly if the input transformer uses bifilar winding in the secondary. Second, dc currents in the transformer secondary are balanced, making the transformer less microphonic. (With a single-ended input, quiescent emitter/source current creates a dc magnetic field in the transformer core. Any vibration will generate signals in the secondary.) Third, it may be easier to build a differential amplifier whose operating point is stable with temperature changes (improved bias stability). And last, any even-harmonic distortion in the input stages cancels. (Odd-harmonic distortion is unaffected.)

In order to retain the good noise figure of the single-ended input circuit, we must be sure that the differential amplifier following the input stages in the differential circuit has good common-mode rejection. If it does not, common-mode noise from the input stages will also be amplified, and the noise figure will be worse than anticipated. This is not usually a severe problem

> *Example:* In the Portable VLF Receiver, common-mode noise (which appears at the input of the receiver as an additional current noise generator) increases I_n by about 7%, or 0.6 dB.

6. Receiver Calibration

6.1 Induced *versus* Injected Calibration

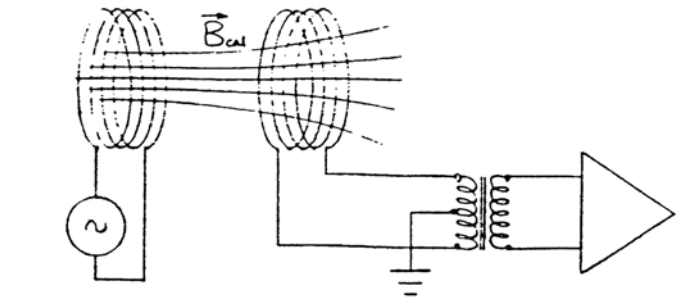

(a) Induced

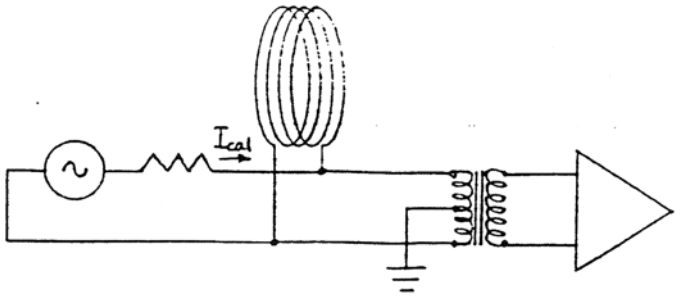

(b) Injected

Figure 6.1. Receiver calibration methods.

In order to make accurate measurements of the strength of received signals it is necessary to determine the response of the VLF receiver to known fields. There are two common ways of doing this. The first method, which is illustrated in Figure 6.1(a), uses a separate calibration coil to generate a known magnetic flux through the VLF antenna. The second method, shown in Figure 6.1(b), uses a signal generator to inject a known current into the VLF receiver input in parallel with the antenna. Other possible injection methods use an additional transformer winding for current injection, or a separate transformer in series with the antenna to insert a known emf into the antenna circuit, but they are all similar.

The induced calibration method would appear to be superior, since we are inducing a signal in the antenna just as if an incident wave were being received, whereas the injected calibration method inserts the signal after the antenna. In fact, they are equally accurate and effective. It is usually impractical to separate the calibration coil far enough from the

receiving antenna to make the field at the antenna truly uniform. In order to calculate the flux from the calibration coil passing through the receiving antenna we must know the geometry and placement of the two loops, especially accurately if they are close together. With the injected calibration method we must know the area of the loop, its number of turns, and impedance, all of which can be measured to the same accuracy as the dimensions needed for the induced calibration calculations. Thus there is little or no difference in accuracy between the two methods.

In the case of ferrite-cored loops, or loops where distributed capacitance or other high-frequency effects are important, the induced calibration method may be superior. In this case we should try to generate as uniform a field through the receiving antenna as possible. If the antenna is fairly small a pair of Helmholz coils may be a good field source. For air-core VLF loops, however, the injected calibration method will be just as accurate, and since it is simpler to perform we shall concentrate on this method.

6.2 Balanced Current Injection

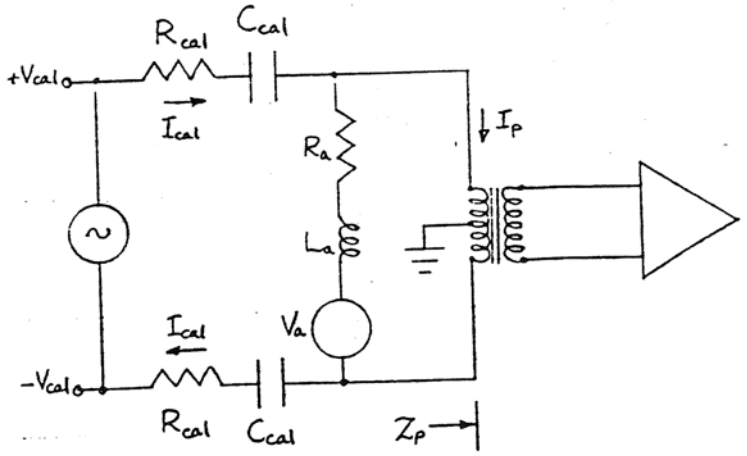

Figure 6.2. Balanced current injection.

Figure 6.2 shows a balanced calibration current I_{cal} injected into the receiver at the antenna terminals by means of two voltages, $+V_{cal}$ and $-V_{cal}$, applied to resistors R_{cal} and capacitors C_{cal}. If R_{cal} is much larger than (half) the impedance seen at the antenna terminals (the parallel combination of Z_a, the antenna impedance, and $Z_p = R_{in}/m^2$, the receiver input impedance at the transformer primary) then I_{cal} will depend only on R_{cal} and C_{cal} and is given by

$$I_{cal} = \frac{V_{cal}}{R_{cal}(1 + f_{cal}/jf)} \tag{6.1}$$

where

$$f_{cal} = 1/(2\pi C_{cal} R_{cal}). \tag{6.2}$$

The current flowing into the receiver input due to V_{cal} is then

$$I_{in} = \frac{V_{cal}}{R_{cal}(1 + f_{cal}/jf)} \cdot \frac{j\omega L_a(1 + f_a/jf)}{R_a + j\omega L_a + Z_p}. \tag{6.3}$$

The current flowing into the receiver due to an antenna emf V_a is

$$I_{in} = \frac{V_a}{R_a + j\omega L_a + Z_p} \tag{6.4}$$

or, using Equation (2.3),

$$I_{in} = \frac{j\omega NAB_w}{R_a + j\omega L_a + Z_p} \tag{6.5}$$

where B_w is the magnetic field of the received wave. Comparing Equations (6.3) and (6.5), we see that the response generated by B_w is the same as that produced by a calibration voltage of magnitude

$$V_{cal} = \frac{NAR_{cal}B_w}{L_a} \cdot \frac{1 + f_{cal}/jf}{1 + f_a/jf}. \tag{6.6}$$

If we choose C_{cal} so that $f_{cal} = f_a$, or

$$C_{cal} = \frac{L_a}{R_a R_{cal}} \tag{6.7}$$

then the frequency-dependent terms in Equation (6.6) cancel, and we have

$$V_{cal} = \frac{NAR_{cal}}{L_a} B_w \tag{6.8}$$

or

$$V_{cal} = \frac{NAR_{cal}}{cL_a} E_w$$

in terms of the equivalent free-space electric field.

The calibration factor NAR_{cal}/L_a depends on the area, number of turns, and inductance of the antenna. It does *not* depend on the input impedance of the amplifier (the terms in Z_p have very neatly canceled out). And as long as we choose C_{cal} correctly, the calibration factor does not depend on frequency. We can determine the frequency response of the receiver by applying a voltage V_{cal} at different frequencies and measuring the receiver output. It may be convenient to replace the actual antenna with a dummy antenna (an inductor and resistor combination with the same impedance as the real antenna but with little or no effective area) in order to get a cleaner output signal.

If the receiver is to be used with various antennas of different areas and numbers of turns, the same calibration circuit can be used, provided that the different antennas have the same impedance. It is only necessary to insert the particular values of N and A into Equation (6.8) to determine the system response for each antenna.

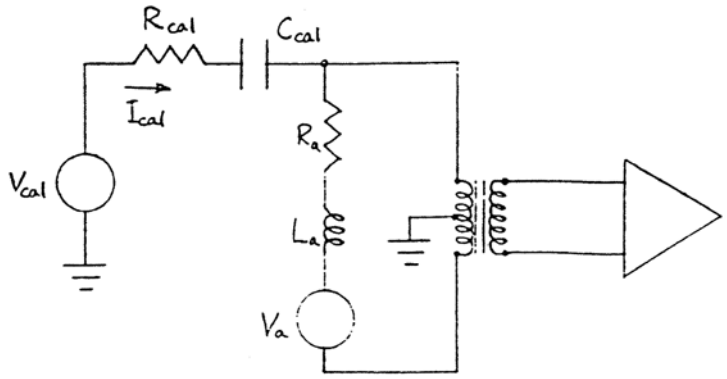

Figure 6.3. Unbalanced current injection.

6.3 Unbalanced Current Injection

Figure 6.3 shows a current injection circuit where an unbalanced current I_{cal} is injected into one of the antenna input terminals. In this case, I_{cal} generates a current through only one half of the input transformer primary, and the calibration factor is one-half that above, or

$$V_{cal} = \frac{NAR_{cal}}{2L_a} B_w = \frac{NAR_{cal}}{2cL_a} E_w. \tag{6.9}$$

As long as the input transformer is well balanced, this method is just as good.

The unbalanced calibration method is more useful when making relative frequency response measurements, since it is hard to find balanced signal generators. However, for absolute gain calibration, particularly if the calibration signal must be applied from the end of a long transmission line between the laboratory and the receiver, the balanced calibration method is preferred since there will be no problem with common-mode signals. If the unbalanced calibration method is used over long lines, care must be taken to ensure that amplified signal currents from the receiver output cannot flow in the calibration circuit (say, through a common ground wire), generating a possible voltage drop between the signal generator and the calibration input and resulting in an incorrect voltage applied at the antenna.

Example: The Portable VLF Receiver uses both methods of calibration. An internal calibration oscillator generates a 5 kHz square-wave signal which is applied to the antenna input to give a balanced calibration current of $I_{cal} = 2.0 \times 10^{-8}$ A rms (5 kHz component). This internal calibration is used to provide an output signal of known amplitude when making field recordings. The dummy loop used with the Portable VLF Receiver has an unbalanced calibration input with $R_{cal} = 10.0$ kΩ, $C_{cal} = 0.10$ μF, for use in making relative frequency response measurements in the laboratory. See Schematic 10.4 for details of the dummy loop.

7. Portable VLF Receiver — Circuits and Operation

Refer to Schematics 9.1 and 9.2 for drawings of the two electronics cards used in the receiver.

7.1 Circuit Description, Card 1

Input Amplifier. The input amplifier consists of transistors Q_1 through Q_7. The antenna signal is coupled through the input transformer T_1 to the emitters of the common-base input amplifiers Q_1 and Q_2. These transistors operate with 100 μA quiescent emitter current, giving $r_e = 260\ \Omega$, or $R_{in} = 520\ \Omega$ emitter-to-emitter. The outputs of Q_1 and Q_2 are amplified by the differential pair Q_3-Q_4, each running at 31 μA emitter current to keep their noise current below that of Q_1 and Q_2. Q_5 and Q_6 are emitter-followers to provide a low-impedance output from the differential amplifier. R_5 and R_6 apply feedback around the differential amplifier to lower its input impedance and set the circuit gain.

Q_7 is a current source for Q_3-Q_4. Common-mode feedback is applied to the base of Q_7 through R_{11}, R_{12}, and R_{15} to increase the common-mode rejection of the circuit. DC common-mode feedback is also applied by R_{17} to the emitters of Q_1 and Q_2 (through the transformer secondary center-tap) to set the operating point of the input amplifiers. A smaller amount of differential dc feedback is applied to the bases of Q_1 and Q_2 through R_9 and R_{10} to equalize the emitter currents of the input amplifiers. The DC BALance potentiometer R_{35} is set to equalize the dc voltages at the emitters of Q_5 and Q_6, thus balancing the input circuit. This is important for good common-mode rejection at lower frequencies, and helps to reduce low-frequency oscillations in the receiver.

Diodes D_1 and D_2 discharge the base bypass capacitors C_1 and C_2 when the receiver is turned off. Otherwise these capacitors would reverse-bias the base-emitter junctions of Q_1 and Q_2 and might cause excessive reverse base current to flow with consequent damage to the input transistors' noise figures. Diode D_3 provides some temperature compensation to the bias point of the circuit.

The dc power to the input stage is filtered by R_{18}-C_5 and R_{20}-C_4 to attenuate power-supply feedback. The voltage to the collector resistors of the differential pair Q_3-Q_4 is further filtered by R_{19}-C_3.

Frequency Compensation Stage. The frequency compensation amplifier U_1 equalizes the receiver gain below f_i (350 Hz) to provide a flat frequency response down to about 60 Hz. It provides a voltage gain of 2 at higher frequencies. The frequency compensation action of U_1 is only used when the front-panel HI-PASS switch is in the "FLAT" position. In the "350 Hz" or "1 kHz" positions analog switch U_4 (pins 3-4) shorts the integrating

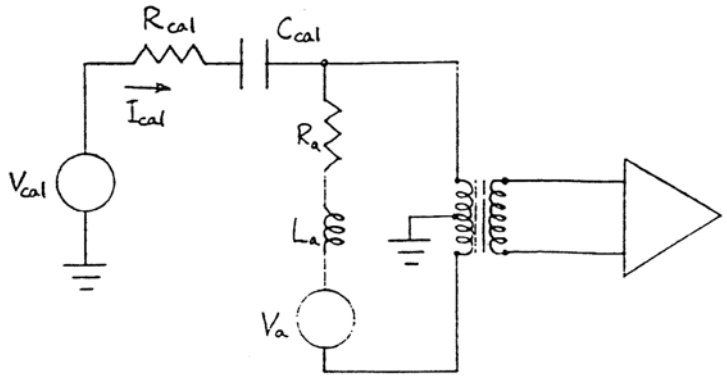

Figure 6.3. Unbalanced current injection.

6.3 Unbalanced Current Injection

Figure 6.3 shows a current injection circuit where an unbalanced current I_{cal} is injected into one of the antenna input terminals. In this case, I_{cal} generates a current through only one half of the input transformer primary, and the calibration factor is one-half that above, or

$$V_{cal} = \frac{NAR_{cal}}{2L_a} B_w = \frac{NAR_{cal}}{2cL_a} E_w. \tag{6.9}$$

As long as the input transformer is well balanced, this method is just as good.

The unbalanced calibration method is more useful when making relative frequency response measurements, since it is hard to find balanced signal generators. However, for absolute gain calibration, particularly if the calibration signal must be applied from the end of a long transmission line between the laboratory and the receiver, the balanced calibration method is preferred since there will be no problem with common-mode signals. If the unbalanced calibration method is used over long lines, care must be taken to ensure that amplified signal currents from the receiver output cannot flow in the calibration circuit (say, through a common ground wire), generating a possible voltage drop between the signal generator and the calibration input and resulting in an incorrect voltage applied at the antenna.

Example: The Portable VLF Receiver uses both methods of calibration. An internal calibration oscillator generates a 5 kHz square-wave signal which is applied to the antenna input to give a balanced calibration current of $I_{cal} = 2.0 \times 10^{-8}$ A rms (5 kHz component). This internal calibration is used to provide an output signal of known amplitude when making field recordings. The dummy loop used with the Portable VLF Receiver has an unbalanced calibration input with $R_{cal} = 10.0$ kΩ, $C_{cal} = 0.10$ μF, for use in making relative frequency response measurements in the laboratory. See Schematic 10.4 for details of the dummy loop.

7. Portable VLF Receiver — Circuits and Operation

Refer to Schematics 9.1 and 9.2 for drawings of the two electronics cards used in the receiver.

7.1 Circuit Description, Card 1

Input Amplifier. The input amplifier consists of transistors Q_1 through Q_7. The antenna signal is coupled through the input transformer T_1 to the emitters of the common-base input amplifiers Q_1 and Q_2. These transistors operate with 100 μA quiescent emitter current, giving $r_e = 260\ \Omega$, or $R_{in} = 520\ \Omega$ emitter-to-emitter. The outputs of Q_1 and Q_2 are amplified by the differential pair Q_3-Q_4, each running at 31 μA emitter current to keep their noise current below that of Q_1 and Q_2. Q_5 and Q_6 are emitter-followers to provide a low-impedance output from the differential amplifier. R_5 and R_6 apply feedback around the differential amplifier to lower its input impedance and set the circuit gain.

Q_7 is a current source for Q_3-Q_4. Common-mode feedback is applied to the base of Q_7 through R_{11}, R_{12}, and R_{15} to increase the common-mode rejection of the circuit. DC common-mode feedback is also applied by R_{17} to the emitters of Q_1 and Q_2 (through the transformer secondary center-tap) to set the operating point of the input amplifiers. A smaller amount of differential dc feedback is applied to the bases of Q_1 and Q_2 through R_9 and R_{10} to equalize the emitter currents of the input amplifiers. The DC BALance potentiometer R_{35} is set to equalize the dc voltages at the emitters of Q_5 and Q_6, thus balancing the input circuit. This is important for good common-mode rejection at lower frequencies, and helps to reduce low-frequency oscillations in the receiver.

Diodes D_1 and D_2 discharge the base bypass capacitors C_1 and C_2 when the receiver is turned off. Otherwise these capacitors would reverse-bias the base-emitter junctions of Q_1 and Q_2 and might cause excessive reverse base current to flow with consequent damage to the input transistors' noise figures. Diode D_3 provides some temperature compensation to the bias point of the circuit.

The dc power to the input stage is filtered by R_{18}-C_5 and R_{20}-C_4 to attenuate power-supply feedback. The voltage to the collector resistors of the differential pair Q_3-Q_4 is further filtered by R_{19}-C_3.

Frequency Compensation Stage. The frequency compensation amplifier U_1 equalizes the receiver gain below f_i (350 Hz) to provide a flat frequency response down to about 60 Hz. It provides a voltage gain of 2 at higher frequencies. The frequency compensation action of U_1 is only used when the front-panel HI-PASS switch is in the "FLAT" position. In the "350 Hz" or "1 kHz" positions analog switch U_4 (pins 3-4) shorts the integrating

capacitor C_7, and U_1 has a gain of 2 at all frequencies. U_1 is used in the non-inverting configuration to provide a high impedance load on the input stage. Note that U_1 is dc-coupled to the input stage, and its output voltage is about -2.8 V dc.

High-Pass Filter. U_2 and U_3 form a *4th*-order 1 kHz Butterworth high-pass filter. The filter is switched in series with the output of the frequency compensation stage when the front-panel HI-PASS switch is in the "1 kHz" position. This is used to attenuate power-line interference in locations where it may be a problem and where good low-frequency response is not important. The analog switches U_4 select either the output of the frequency compensation state, or the output of the filter, as the output of Card 1.

7.2 Circuit Description, Card 2

Variable Gain Amplifier. The variable gain amplifier consists of amplifier U_{101} and analog switches U_{102}. Depending on the front-panel GAIN switch settings, U_{102} adjusts the feedback around U_{101} to set the gain of the amplifier to be 0, 20, or 40 dB. Note that the signal ground return (Card 2, pin 22) is obtained from Card 1, preventing ground-loop feedback between the two cards. C_{101} provides dc feedback around U_{101} to ensure bias stability even at 40 dB ac gain.

Output Amplifier. The LEVEL control on the front panel attenuates the signal from the variable gain amplifier, and sends it to the output amplifier U_{103}. This amplifier provides an additional 10 dB gain and a low-impedance output (at the OUTPUT connector) for external use. However, see Section 7.4 below for permissible loads.

Speaker Amplifier. The speaker amplifier provides enough power to drive a loudspeaker. The signal from the variable gain amplifier is attenuated by the VOLUME control and amplified by U_{104}, which is followed by the complementary current amplifier transistors Q_{101}-Q_{102}. Feedback resistors R_{113} and R_{114} set the voltage gain to about 9 dB. Diodes D_{101} and D_{102} set the bias voltage for Q_{101}-Q_{102}, and R_{118} and R_{119} determine the quiescent current of Q_{101}-Q_{102}. Diodes D_{103} and D_{104} bypass R_{118} and R_{119} at high current to provide good power output. R_{117} and R_{120} limit the maximum continuous battery current that can be consumed. Capacitors C_{111} and C_{112} filter the power applied to Q_{101} and Q_{102} to attenuate power-supply feedback. Note that the grounds of C_{111} and C_{112} are made by a separate connection to the speaker ground; this is done to prevent high-current ground loops.

Calibration Oscillator. U_{105} is a multivibrator running at 5 kHz that generates a differential square-wave signal used for receiver gain calibration. When the front-panel CAL button is pressed, power is applied to U_{105} through R_{121} and zener diode D_{105}, which serve to keep the oscillator output voltage constant even though the battery voltage

may vary. The output of the oscillator is attenuated by the balanced attenuator R_{123} through R_{130}, and applied through the calibration resistors R_{33} and R_{34} (Card 1) to inject a balanced calibration current of $I_{cal} = 2.0 \times 10^{-8}$ A rms (5 kHz component). The calibration attenuator CAL LEVEL potentiometer R_{125} should be adjusted so that the voltage at the cal test point is 1.00 volt peak-to-peak.

Battery Test Circuit. When the BATT TEST button is depressed, current through D_{106} turns on Q_{103}, and lights the front-panel battery test light if the total battery voltage available is greater than 10.7 V. This is the minimum voltage for receiver operation. Total supply voltage with new batteries is about 15 V.

7.3 Hints to Successful Receiver Operation

The operation of the Portable VLF Receiver is straightforward, but the following comments may be some help.

The most important factor in obtaining good performance lies in the location of the receiving site. Select a site away from local power lines to reduce hum interference, especially if low-frequency measurements are to be made. In areas where interference is a problem, re-orienting the loop antenna may decrease the hum level. It may be necessary to use the built-in high-pass filter in very noisy areas.

Good connections to the antenna and input terminals are important. Any resistance in the antenna lead-in wires or at the terminals appears in series with the antenna resistance R_a (approximately 1 Ω). Additional resistance will generate additional noise at low frequencies and degrade the receiver frequency response at the low end. If the lead-in wires are longer than a foot or so, they should be shielded and the shield connected to the receiver ground terminal.

When operating with high gain and volume settings, the receiver may exhibit low-frequency oscillations when the HI-PASS switch is in the "FLAT" position. This is due to high battery current to the speaker causing internal power supply bus feedback. This is more likely to be a problem where strong low-frequency signals such as hum are present. Either reduce the volume or use high-impedance (600 Ω) headphones to monitor reception.

Use the internal CAL signal when making field tape recordings to provide a reference signal on the tape. The calibration oscillator injects a square-wave current into the antenna terminals whose 5 kHz component is 2.0×10^{-8} A rms. The equivalent wave intensity of the cal signal for a given antenna can be calculated from

$$B_w = \frac{L_a}{NA} I_{cal} \qquad \text{or} \qquad E_w = \frac{cL_a}{NA} I_{cal}. \tag{7.1}$$

The calibration-equivalent fields for the standard 1 Ω/1 mHy antennas are shown in Table 7.1. See Table 3.3 for other details of these antennas.

Table 7.1. Calibration-Equivalent Fields for Standard Antennas

Shape	Size, side or base	Wire AWG	N	L_a mHy	A m^2	B_{cal} T	E_{cal} V m^{-1}
square	16.0 cm	20	47	0.998	0.02563	1.66×10^{-11}	4.97×10^{-3}
	56.7 cm	18	21	0.994	0.3219	2.94×10^{-12}	8.81×10^{-4}
	1.70 m	16	11	1.013	2.892	6.37×10^{-13}	1.91×10^{-4}
	4.90 m	14	6	1.029	24.05	1.43×10^{-13}	4.27×10^{-5}
right	2.60 m	16	12	1.005	1.695	9.88×10^{-13}	2.96×10^{-4}
isosceles	8.39 m	14	6	0.996	17.59	1.89×10^{-13}	5.66×10^{-5}
triangle	27.3 m	12	3	0.967	187.0	3.45×10^{-14}	1.03×10^{-5}
	60.7 m	10	2	1.043	920.9	1.13×10^{-14}	3.39×10^{-6}
	202 m	8	1	0.995	10164	1.96×10^{-15}	5.87×10^{-7}

The equivalent fields B_{cal} and E_{cal} listed assume a calibration current of $I_{cal} = 2.0 \times 10^{-8}$ A rms. This is the amplitude of the 5-kHz component of the internal calibration source in the Portable VLF Receiver.

Use the BATTery TEST button to check battery voltage. If the test light does not come on, the batteries must be replaced. The receiver requires 10 each "D" cells.

7.4 Driving Long Lines from the Output Jack

The output signal BNC jack on the Portable VLF Receiver is driven by output amplifier U_{103}, a type 741 op-amp. The drive capability of the op-amp determines the minimum load impedance that can be connected to the receiver output. The op-amp will clip and distort large signals if the load resistance is less than 2 kΩ. The output circuit may also become unstable and oscillate if a capacitive load is connected. A long coaxial cable can be used to connect the receiver to a tape recorder (or other load) if the following points are kept in mind:

1. Use a cable with a relatively high impedance. RG62/U (93 Ω) is better than RG59/U (73 Ω), which itself is preferable to RG58/U (50 Ω).
2. The cable should be terminated at the far end by a resistor approximately equal to the cable impedance (say, 100 Ω for RG62/U) if the cable is very long. This will ensure that the cable looks like a resistor rather than a capacitor at the receiver end, and will give the best frequency response.
3. The simplest way to drive the cable is through a 2 kΩ resistor in series with the receiver output. The series resistor limits the current out of the receiver to prevent distortion. However, this resistor together with the load resistance of the cable form a

voltage divider, and only a small part of the signal (say, 1/21*st* for a 100 Ω terminated cable) appears at the cable end.

4. A more complicated way to drive the cable would be through a matching transformer with a turns ratio of 5:1 or greater. This would raise the 100 Ω impedance of the terminated cable to at least 2000 Ω as seen by the receiver output. A 100 Ω series resistor may be needed between the receiver output jack and the transformer to prevent high-frequency (several hundred kilohertz) oscillations caused by the distributed capacitance of the transformer windings.

8. Portable VLF Receiver — Measurement of Performance

8.1 Gain and Frequency Response

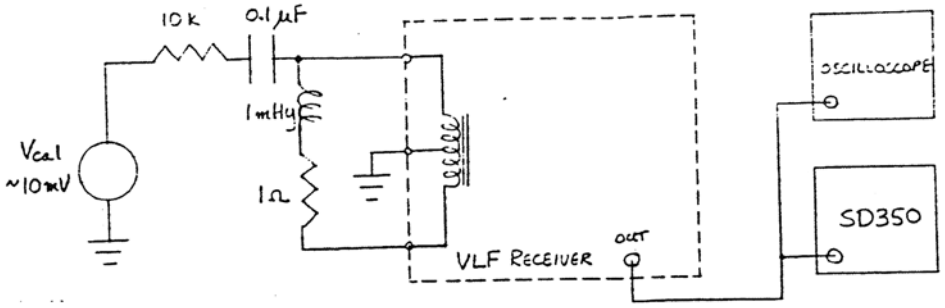

Figure 8.1. Gain measurement.

Figure 8.1 shows the instrument connections for gain measurement. A 10 mV signal is applied to the unbalanced calibration input of the dummy loop. The output of the receiver is monitored on an oscilloscope, and measured on a spectrum analyzer (the Spectral Dynamics SD350 is recommended). Receiver settings should be:

GAIN = 20 dB

LEVEL = max clockwise

The receiver gain should be measured for each position of the HI-PASS switch. The calibration gain G is calculated from

$$G = \frac{V_{out}}{V_{cal}}. \tag{8.1}$$

The cal gain of the prototype model is about 31 dB at the center of the frequencies of interest. Relative frequency response (gain with respect to the gain at middle frequencies) is shown in Figure 8.3.

8.2 Noise and Sensitivity

The setup for noise measurement is the same as that for gain measurement, Figure 8.1, except that the calibration oscillator is not used. GAIN and LEVEL settings are as above. When making noise measurements it is important to situate the receiver and dummy loop to minimize local hum pickup which might otherwise saturate the spectrum analyzer. It may help to use magnetic shielding around the receiver, such as putting it in a steel wastebasket. The output noise density E_{no} is divided by the calibration gain G (measured above) at each particular frequency to find the noise referred to the input by

$$E_{ni} = E_{no}\frac{\omega L_a}{2R_{cal}G}. \tag{8.2}$$

The measured noise factor is then

$$F = \frac{E_{ni}^2}{E_a^2} \tag{2.21}$$

where $E_a^2 = 1.61 \times 10^{-20}$ V^{2}Hz^{-1}. The system sensitivity for a given antenna can be found from

$$S_{sys} = S_0\sqrt{F}/f \tag{2.22}$$

where S_0 is the normalized sensitivity of the antenna (see Table 3.3).

The receiver noise fiqure can be calculated theoretically from the noise model in Section 2.9 by using Equation (2.36). For the Portable VLF Receiver we have the following values:

$m = 22.8$	$p = 1.122$
$R_a = 1\ \Omega$	$E_n = 2.87 \times 10^{-9}$ V Hz$^{-1/2}$
$f_a = 159.2$ Hz	$I_n = 4.44 \times 10^{-13}$ A Hz$^{-1/2}$
$R_p = 0.039\ \Omega$	$f_{tn} = 18$ Hz
$R_s = 20.2\ \Omega$	$f_{cn} = 6480$ Hz

giving

$$F = 2.333 + \left(\frac{2.40\text{ Hz}}{f}\right)^2 + \left(\frac{f}{1995\text{ Hz}}\right)^2 + \left(\frac{f}{6506\text{ Hz}}\right)^4. \tag{8.3}$$

The measured and calculated noise figures, and sensitivities with the 56.7 cm square loop, are shown in Figures 8.4 and 8.5. (See also Figure 2.11).

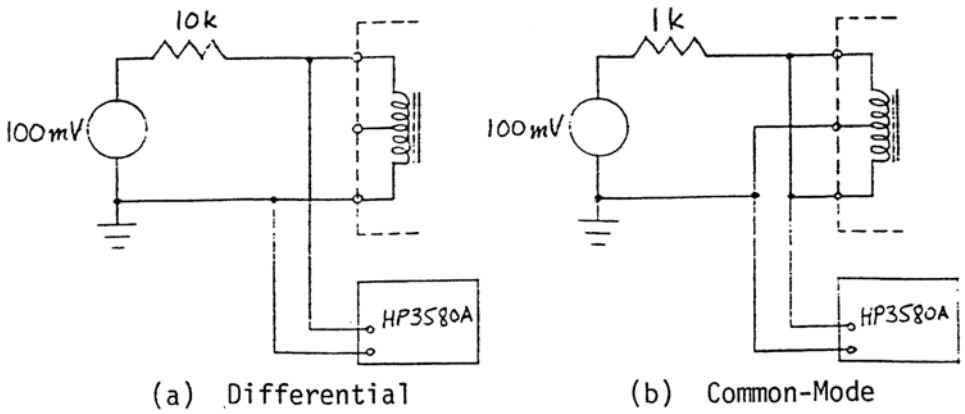

Figure 8.2. Input impedance measurement.

8.3 Input Impedance

The differential and common-mode input impedance are each measured as shown in Figures 8.2(a) and 8.2(b). A known current is applied to the input terminals, and the voltage across the receiver input is measured with a spectrum analyzer (Hewlett-Packard 3580A recommended).

Note that in the differential measurement one of the input terminals is grounded. It is important not to ground the case of the receiver (which is at a potential mid-way between the input terminals) for this measurement. Figure 8.6 shows the results. The differential input impedance decreases at low frequencies where the shunting effect of L_p becomes important, and increases at high frequencies due to L_2. The common-mode input impedance is low throughout.

8.4 Common-Mode Rejection

The common-mode gain for a current input is measured by injecting a known current as in Figure 8.2(b) and measuring the output produced. The differential gain for a current input can be calculated from the cal gain G measured in Section 8.1 by multiplying G by R_{cal}. The common-mode rejection ratio is defined by

$$\text{CMRR} = \frac{\text{differential gain}}{\text{common-mode gain}}. \tag{8.4}$$

CMRR is shown in Figure 8.7. The CMRR is very sensitive to input transformer balance and wiring layout. The measurements shown were made on the prototype receiver and may be different with other units.

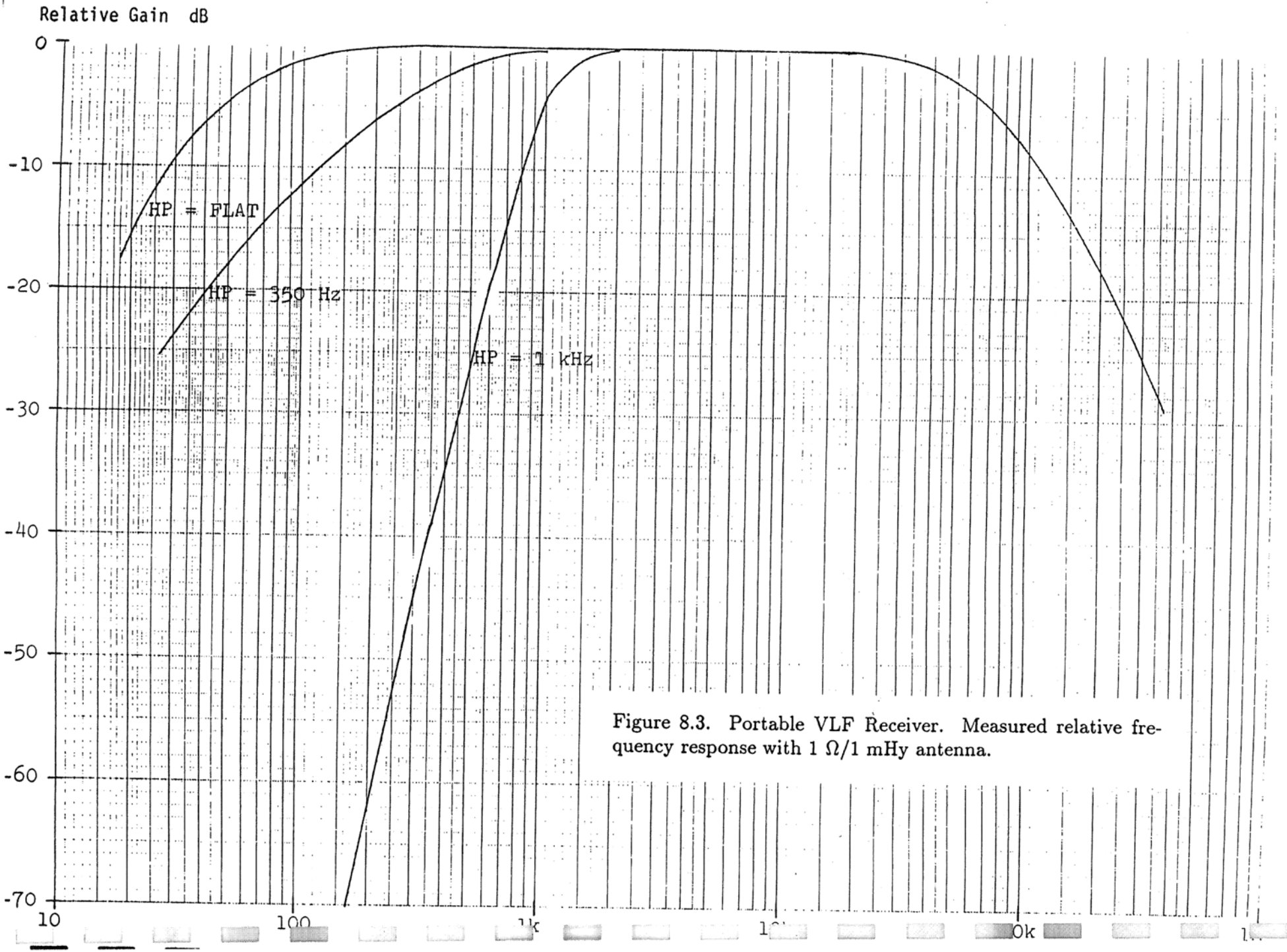

Figure 8.3. Portable VLF Receiver. Measured relative frequency response with 1 Ω/1 mHy antenna.

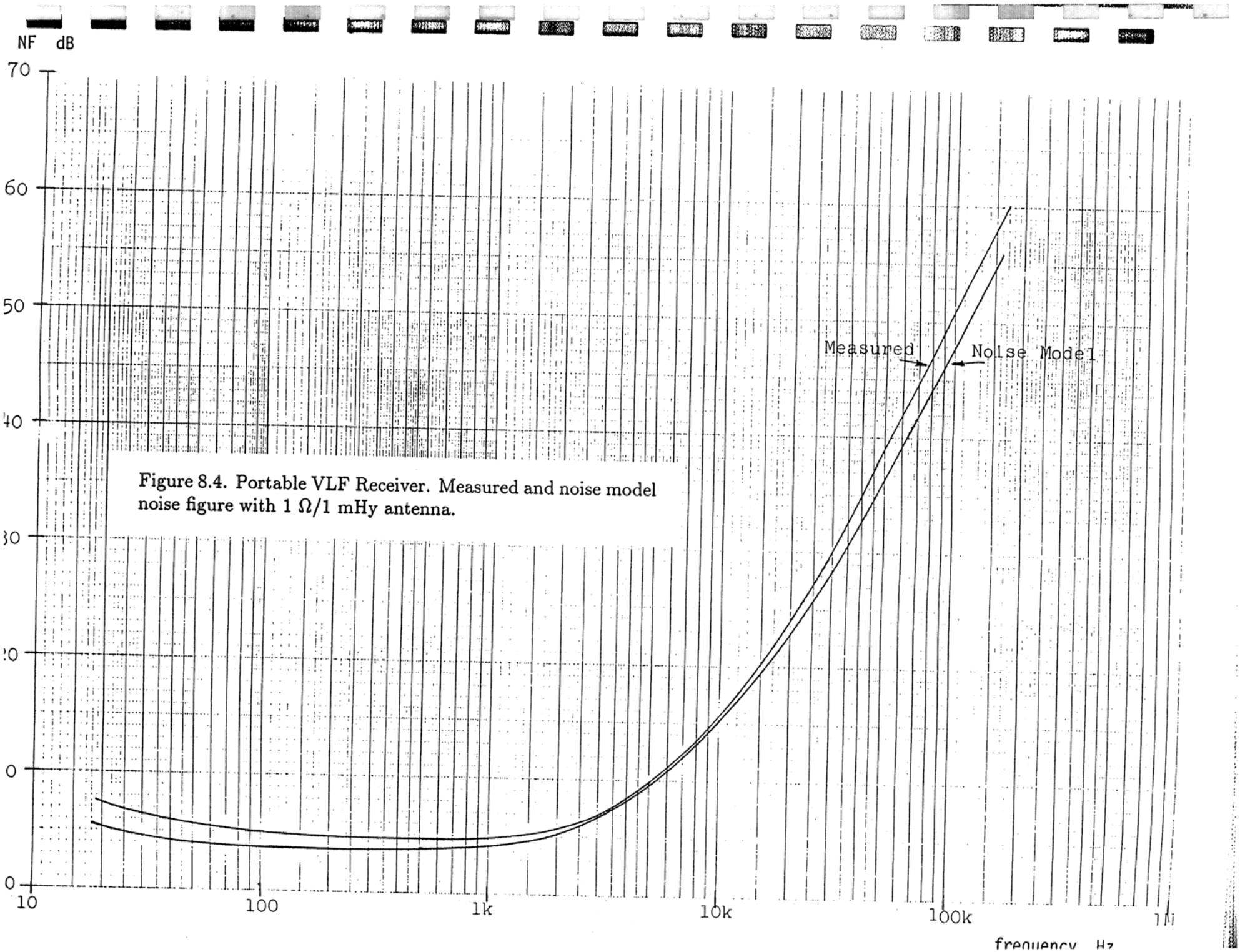

Figure 8.4. Portable VLF Receiver. Measured and noise model noise figure with 1 Ω/1 mHy antenna.

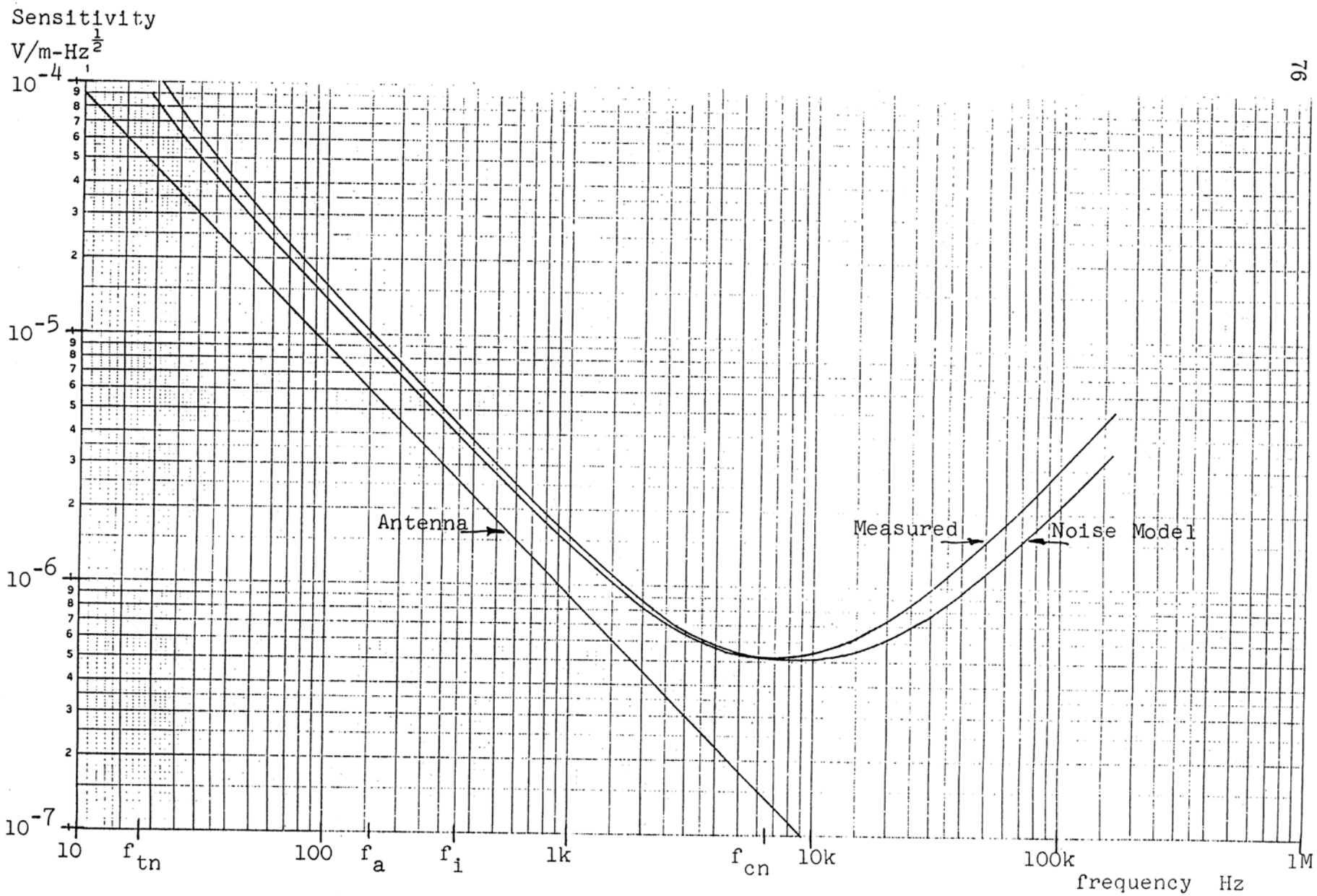

Figure 8.5. Portable VLF Receiver. Measured and noise model sensitivity with 56.7 cm square 1 Ω/1 mHy antenna.

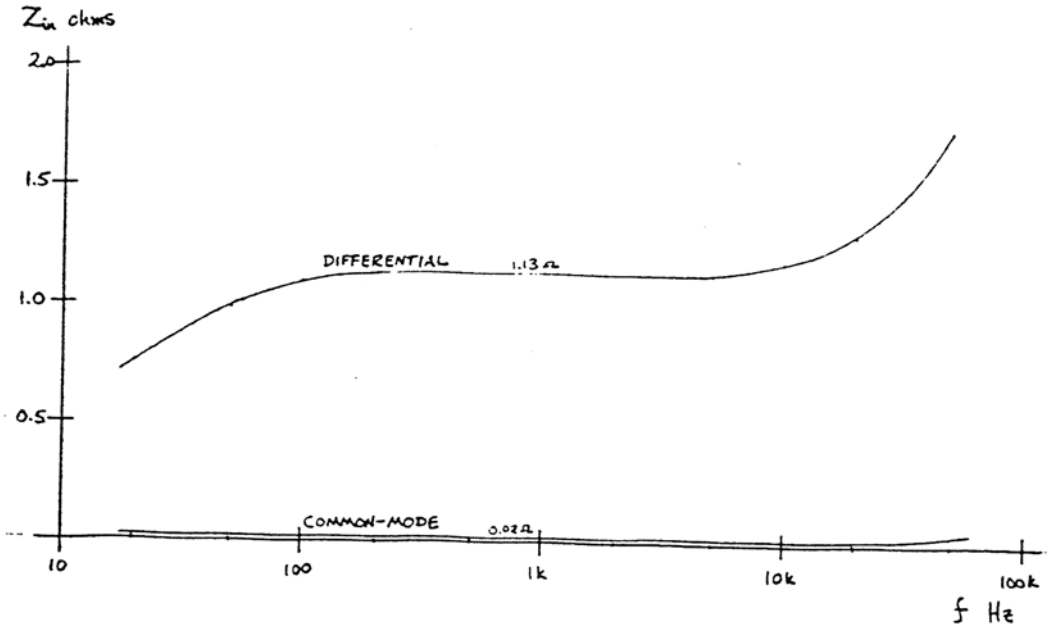

Figure 8.6. Input impedance.

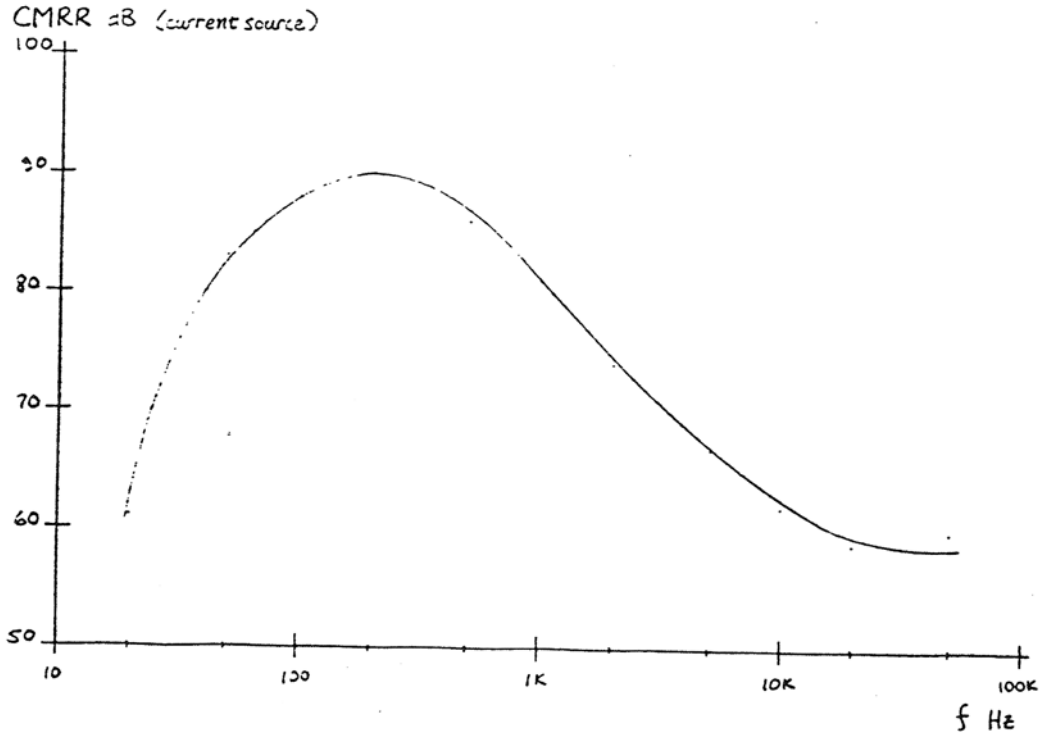

Figure 8.7. Common-mode rejection ratio.

9. Portable VLF Receiver — Parts and Schematics

Resistors

R_1	154 kΩ, 1/4 W, 1% metal film, RN55D
R_2	154 kΩ, 1/4 W, 1% metal film, RN55D
R_3	110 kΩ, 1/4 W, 1% metal film, RN55D
R_4	110 kΩ, 1/4 W, 1% metal film, RN55D
R_5	267 kΩ, 1/4 W, 1% metal film, RN55D
R_6	267 kΩ, 1/4 W, 1% metal film, RN55D
R_7	100 kΩ, 1/4 W, 1% metal film, RN55D
R_8	100 kΩ, 1/4 W, 1% metal film, RN55D
R_9	1.00 MΩ, 1/4 W, 1% metal film, RN55D
R_{10}	1.00 MΩ, 1/4 W, 1% metal film, RN55D
R_{11}	39.2 kΩ, 1/4 W, 1% metal film, RN55D
R_{12}	39.2 kΩ, 1/4 W, 1% metal film, RN55D
R_{13}	25.5 kΩ, 1/4 W, 1% metal film, RN55D
R_{14}	25.5 kΩ, 1/4 W, 1% metal film, RN55D
R_{15}	5.62 kΩ, 1/4 W, 1% metal film, RN55D
R_{16}	39.2 kΩ, 1/4 W, 1% metal film, RN55D
R_{17}	1.82 kΩ, 1/4 W, 1% metal film, RN55D
R_{18}	750 Ω, 1/4 W, 5% carbon composition
R_{19}	7.5 kΩ, 1/4 W, 5% carbon composition
R_{20}	820 Ω, 1/4 W, 5% carbon composition
R_{21}	27.4 kΩ, 1/4 W, 1% metal film, RN55D
R_{22}	27.4 kΩ, 1/4 W, 1% metal film, RN55D
R_{23}	267 kΩ, 1/4 W, 1% metal film, RN55D
R_{24}	10.0 kΩ, 1/4 W, 1% metal film, RN55D
R_{25}	11.5 kΩ, 1/4 W, 1% metal film, RN55D
R_{26}	4.12 kΩ, 1/4 W, 1% metal film, RN55D
R_{27}	26.7 kΩ, 1/4 W, 1% metal film, RN55D
R_{28}	1.0 MΩ, 1/4 W, 5% carbon composition
R_{29}	1.0 MΩ, 1/4 W, 5% carbon composition
R_{30}	100 kΩ, 1/4 W, 5% carbon composition
R_{31}	100 kΩ, 1/4 W, 5% carbon composition
R_{32}	100 kΩ, 1/4 W, 5% carbon composition
R_{33}	10.0 kΩ, 1/4 W, 1% metal film, RN55D
R_{34}	10.0 kΩ, 1/4 W, 1% metal film, RN55D
R_{35}	500 Ω, cermet trimmer, Allen-Bradley D4D501

Resistors, cont.

R_{101}	110 kΩ, 1/4 W, 1% metal film, RN55D
R_{102}	182 kΩ, 1/4 W, 1% metal film, RN55D
R_{103}	18.2 kΩ, 1/4 W, 1% metal film, RN55D
R_{104}	2.00 kΩ, 1/4 W, 1% metal film, RN55D
R_{105}	100 kΩ, 1/4 W, 5% carbon composition
R_{106}	100 kΩ, 1/4 W, 5% carbon composition
R_{107}	100 kΩ, 1/4 W, 5% carbon composition
R_{108}	100 kΩ linear pot, Allen Bradley WA2G056S-104UA
R_{109}	100 kΩ cw log pot, Allen Bradley JA1N200P-104AA
R_{110}	10.0 kΩ, 1/4 W, 1% metal film, RN55D
R_{111}	22.1 kΩ, 1/4 W, 1% metal film, RN55D
R_{112}	27 kΩ, 1/4 W, 5% carbon composition
R_{113}	75 kΩ, 1/4 W, 5% carbon composition
R_{114}	39 kΩ, 1/4 W, 5% carbon composition
R_{115}	1.0 kΩ, 1/4 W, 5% carbon composition
R_{116}	1.0 kΩ, 1/4 W, 5% carbon composition
R_{117}	100 Ω, 1/4 W, 5% carbon composition
R_{118}	100 Ω, 1/4 W, 5% carbon composition
R_{119}	100 Ω, 1/4 W, 5% carbon composition
R_{120}	100 Ω, 1/4 W, 5% carbon composition
R_{121}	1.2 kΩ, 1/4 W, 5% carbon composition
R_{122}	200 kΩ, 1/4 W, 1% metal film, RN55D
R_{123}	39.2 kΩ, 1/4 W, 1% metal film, RN55D
R_{124}	39.2 kΩ, 1/4 W, 1% metal film, RN55D
R_{125}	5 kΩ, cermet trimmer, Allen-Bradley D4D502
R_{126}	8.66 kΩ, 1/4 W, 1% metal film, RN55D
R_{127}	49.9 kΩ, 1/4 W, 1% metal film, RN55D
R_{128}	49.9 kΩ, 1/4 W, 1% metal film, RN55D
R_{129}	22.1 Ω, 1/4 W, 1% metal film, RN55D
R_{130}	22.1 Ω, 1/4 W, 1% metal film, RN55D
R_{131}	2.2 kΩ, 1/4 W, 5% carbon composition
R_{132}	5.6 kΩ, 1/4 W, 5% carbon composition
R_{133}	2.7 kΩ, 1/4 W, 5% carbon composition
R_{134}	10 kΩ, 1/4 W, 5% carbon composition
R_{201}	10.0 kΩ, 1/4 W, 1% metal film, RN55D
R_{202}	1 Ω, 5%, RC20
R_{203}	3.9–4.7 Ω selected, 1/4 W, 5% carbon composition

Capacitors

C_1	40 μF, 10 WVDC, tantalum, Sprague 150D406X9010B
C_2	40 μF, 10 WVDC, tantalum, Sprague 150D406X9010B
C_3	40 μF, 10 WVDC, tantalum, Sprague 150D406X9010B
C_4	40 μF, 10 WVDC, tantalum, Sprague 150D406X9010B
C_5	40 μF, 10 WVDC, tantalum, Sprague 150D406X9010B
C_6	0.47 μF, low voltage Z5U ceramic
C_7	0.010 μF, 5%, Mylar
C_8	0.015 μF, 5%, Mylar
C_9	0.015 μF, 5%, Mylar
C_{10}	0.015 μF, 5%, Mylar
C_{11}	0.015 μF, 5%, Mylar
C_{12}	0.1 μF, 16 WVDC disc ceramic
C_{13}	0.1 μF, 16 WVDC disc ceramic
C_{14}	100 μF, 16 WVDC, aluminum, Sprague TE1162
C_{15}	100 μF, 16 WVDC, aluminum, Sprague TE1162
C_{16}	0.1 μF, 16 WVDC disc ceramic
C_{17}	0.05 μF, 20 WVDC disc ceramic
C_{18}	0.05 μF, 20 WVDC disc ceramic
C_{19}	10 pF, mica
C_{20}	10 pF, mica
C_{21}	0.05 μF, 20 WVDC disc ceramic
C_{22}	0.05 μF, 20 WVDC disc ceramic
C_{101}	2.2 μF, low voltage Z5U ceramic
C_{102}	0.1 μF, 16 WVDC disc ceramic
C_{103}	0.1 μF, 16 WVDC disc ceramic
C_{104}	5 pF, mica
C_{105}	0.1 μF, 16 WVDC disc ceramic
C_{106}	0.1 μF, 16 WVDC disc ceramic
C_{107}	100 pF, mica
C_{108}	0.1 μF, 16 WVDC disc ceramic
C_{109}	10 pF, mica
C_{110}	43 pF, mica
C_{111}	100 μF, 16 WVDC, aluminum, Sprague TE1162
C_{112}	100 μF, 16 WVDC, aluminum, Sprague TE1162
C_{113}	220 pF, mica, selected
C_{114}	0.05 μF, 20 WVDC disc ceramic
C_{115}	0.05 μF, 20 WVDC disc ceramic
C_{201}	0.10 μF, 5%, Mylar

Semiconductors

D_1	1N4148, silicon signal diode
D_2	1N4148, silicon signal diode
D_3	1N4148, silicon signal diode
D_{101}	1N4148, silicon signal diode
D_{102}	1N4148, silicon signal diode
D_{103}	1N4148, silicon signal diode
D_{104}	1N4148, silicon signal diode
D_{105}	1N5239B, zener diode, 9.1 V, 5%
D_{106}	1N5240B, zener diode, 10 V, 5%
D_{107}	light-emitting diode, red, Hewlett-Packard 5082-4655
Q_1	2N4250A, pnp silicon transistor, low-noise
Q_2	2N4250A, pnp silicon transistor, low-noise
Q_3	2N4250A, pnp silicon transistor, low-noise
Q_4	2N4250A, pnp silicon transistor, low-noise
Q_5	2N4250A, pnp silicon transistor, low-noise
Q_6	2N4250A, pnp silicon transistor, low-noise
Q_7	2N4250A, pnp silicon transistor, low-noise
Q_{101}	2N3568, npn silicon transistor
Q_{102}	2N3645, pnp silicon transistor
Q_{103}	2N3568, npn silicon transistor
U_1	CA3140T, op-amp
U_2	μA741C, op-amp
U_3	μA741C, op-amp
U_4	CD4016BE, quad analog switch
U_{101}	LM318N, op-amp
U_{102}	CD4016BE, quad analog switch
U_{103}	μA741C, op-amp
U_{104}	LM301AN, op-amp
U_{105}	CD4047BE, multivibrator

Pot-Core Components, all parts from Magnetics, Inc.

1 ea.	F43428-UG, pot core (input transformer T_1)
1 ea.	B3428-01, bobbin
1 ea.	C3428-17, mounting clamp
1 ea.	G41811-40, pot core (dummy loop L_{201})
1 ea.	B1811-01, bobbin
1 ea.	TC-F1812-C2, tuning core
1 ea.	TB-P1812-A, tuning base
1 ea.	W1811-18, fibre washer
1 ea.	C1811-11, mounting clamp

Miscellaneous

1 ea.	DPDT switch, ALCO MTA-206N
2 ea.	DP3T (special pinout) switch, ALCO MTA-206PA
2 ea.	pushbutton switch, ALCO MSPS-103C
1 ea.	knob, ALCO KN-500BA
1 ea.	knob, ALCO KN-701BA
1 ea.	phone jack, Switchcraft 12A
2 ea.	BNC jack, Amphenol UG625B/U
3 ea.	binding post, Superior Electric DF30 (2 red/1 black)
3 ea.	banana plug, 6-32 screw, Pomona 3265 (dummy loop)
2 ea.	card socket, Vector R644
10 ea.	3-pin transistor socket
6 ea.	8-pin DIP socket, Augat 508-AG10D
3 ea.	14-pin DIP socket, Augat 514-AG10D
10 ea.	single "D" battery holder
10 ea.	size "D" flashlight battery
1 ea.	3-inch loudspeaker, 16–45 Ω impedance (45 Ω preferred)
1 ea.	aluminum cabinet, Moduline MCLS 5-9-9 plus SPH 5-9
1 ea.	minibox (dummy loop), Pomona 2417
2 ea.	printed circuit cards, either Douglas 11-DE-1 or custom-made boards

Total parts cost: approximately $200 (1980 prices).

10. References

The following references are useful sources for further information.

Grossner, Nathan R., *Transformers for Electronic Circuits,* McGraw-Hill, New York, 1983. This is the best book on transformer design, including power and pulse transformers and inductors as well as coupling transformers, and goes into more detail than most of us will ever need.

Helliwell, Robert A., *Whistlers and Related Ionospheric Phenomena,* Stanford University Press, Stanford, CA, 1965. Though magnetospheric research has advanced over the 23 years since this monograph was written, it is still an excellent introduction to natural VLF radio signals.

Magnetics, Inc., *Ferrite Cores for Power and Filter Applications,* 1987. Available from Magnetics, Inc., 900 E. Butler Road, Butler, PA 16003, telephone (412) 282-8282, and its local distributors. This is a catalog of pot cores and accessories, and contains much useful design information. Similar ferrite pot cores are also available from other manufacturers.

Motchenbacher, C. D., and F. C. Fitchen, *Low-Noise Electronic Design,* John Wiley and Sons, New York, 1973. This is the best guide to low-noise audio-frequency circuit design, and contains noise specifications for many different semiconductor devices.

Rheinfelder, William A., *Design of Low-Noise Transistor Input Circuits,* Hayden, New York, 1964. This has a good discussion of noise figure and its measurement, though some of the circuit examples are a bit dated.

Terman, Frederick E., *Radio Engineers' Handbook,* McGraw-Hill, New York, 1943. Don't be put off by the date; this is must bedside reading for electrical engineers. In particular, Terman's inductance formulas are second to none.

Watt, Arthur D., *VLF Radio Engineering,* Pergamon Press, Oxford, 1967. All you want to know, and more, about VLF radio. The emphasis is on communications and narrowband systems, but the section on receiving antennas is pertinent.